

# 20<sup>th</sup> IGS Annual Lecture

## About the Author



Prof. M.R. Madhav, who delivered the twentieth annual lecture of the IGS, graduated from Andhra University in 1960. Subsequently, he obtained the Master's and Doctor of Philosophy degrees from the Indian Institute of Science, Bangalore in the years 1961 and 1968 respectively. At I.I.Sc., he was recipient of the Senior Research Fellowship of the C.S.I.R. and the Burmah Shell Fellowship. He also worked as Scientific Officer during 1965-1967. Since 1967 he has been with the Indian Institute of Technology, Kanpur, where he is credited with

the development and fostering of the post graduate~ program in Geotechnical Engineering.

Prof. Madhav was a Post Doctoral fellow at the University of Sydney, Sydney, Australia during 1970-71, to which place he returned for few months in 1975 as a Visiting Fellow. He was a Visiting Professor (1985-87), Visiting Scientist (1988 May to July) and Adjunct Professor (1988-1993) at Concordia University, Montreal, Canada. Prof Madhav was the first professor (1992 & 1993) to be appointed at the newly started Institute of Lowland Technology, Saga University, Saga, Japan. He returned to this place in 1997 (August to Dec.) as a Guest Professor. He also was a Visiting Professor at the University of Ghent, Ghent, Belgium, during the summers of 1991 and 1995. He was also an Associate at the International Centre for Theoretical Physics, Trieste, Italy. During his stay at Saga, he organised very successfully the International Symposium on Problems of Lowland Development in Nov. 1992 and co-edited a book entitled "LOWLANDS - DEVELOPMENT AND MANAGEMENT".

Prof. Madhav guided more than 15 doctoral theses in India and three abroad, several masters' and final year projects. He has more than 200 publications out of which about 80 are in International and National journals. He has chaired technical sessions in many international conferences, was a Panellist in the XIII International Conference on Soil Mechanics and Foundation Engineering, New Delhi,

1994, and was member of the Organising Committee of IS Kyushu 1992 and 1996 and delivered lectures all over the world.

Prof. Madhav was elected a Fellow of the National Academy of Engineering with effect from Jan. 1996, and awarded the Prof. Mehra National Research Award of the University of Roorkee also 1996. He is a Life Fellow of the IGS and the Institution of Engineers (India) and was recipient of prizes from these two societies. He also received awards from the Central Board of Irrigation and Power, New Delhi. Presently, he is the Chairman of the IGS Local Chapter at Kanpur.

Prof. Madhav was instrumental in developing many new courses to name a few, Settlement Analysis of Foundations, Engineering of Ground, etc., at I.I.T., Kanpur. He has organised several Intensive and Short Term courses to Teachers from Engineering Colleges and practising Engineers. Major areas of his research are analysis of foundations, ground improvement techniques, application of geosynthetics, etc. and in particular modelling of complex ground engineering problems. His lecture this year would highlight his contributions in this field.

## **Chairman's Remarks**

Prof. A.V. Shroff, Chairman, Baroda Chapter of IGS welcomed the gathering and introduced the Chairman of the Session.

The Chairman Prof. A. Sridharan, a distinguished Geotechnical Engineer and President of Indian Geotechnical Society, introduced the speaker of the session, Prof. M.R. Madhav.

He introduced Prof. Madhav as an educator and eminent research worker, who has actively participated in several national and international activities to promote geotechnical engineering. Making special mention about the role of modelling in ground engineering, he requested Prof. Madhav to deliver the IGS Lecture.

Prof. Madhav began the lecture with the following remarks :

*"Prof. Sridharan, President of IGS, Prof. A.V. Shroff, Chairman, IGC-97, distinguished delegates, ladies and gentlemen.*

*I feel greatly honoured for having been invited to deliver the IGS Annual Lecture. I take this opportunity to thank the Indian Geotechnical Society."*

Prof. Madhav delivered the 20<sup>th</sup> Annual Lecture on "Modelling and Analysis in Geotechnical/Ground Engineering". The text of the lecture appears as an article in this issue of the Journal.

## **Vote of Thanks**

Dr. K.S. Rao, Honorary Secretary of the Indian Geotechnical Society proposed a vote of thanks.

## **Modelling and Analysis in Geotechnical/Ground Engineering\***

**Madhira R Madhav†**

Mizu utte Watering the garden –  
tsuchi no sasayaki I listen to the whispering  
kiku yamiyo. of soil in the dark.

*(Mariane Bozin & translated by Uchida)*

So far as the law of mathematics refer to reality, they are not certain.  
And so far as they are certain, they do not refer to reality.

*(Einstein in Geometry and Experience)*

A model is, and must be, unrealistic in the sense in which the word is most commonly used. Nevertheless, and in a sense paradoxically, if it is a good model it provides the key to understanding reality.

*(Baran and Sweezy, 1968)*

### **Modelling**

**M**odelling can be defined as representation of some aspect of real behaviour, a situation or a problem (soil/foundation) by a more abstract system. Mathematics provides a broad framework for modelling with its well established rules and properties. Once the real behaviour is identified with a branch or certain aspect of mathematics, one can exploit the features embedded in that formulation and derive predictions. The predictions are compared with observation data, and if they do not confirm with the latter, the model is rejected, modified or improved.

---

\* Twentieth IGS Annual Lecture delivered on the occasion of 39<sup>th</sup> Annual General Session held at Baroda.

† Professor of Civil Engineering, Indian Institute of Technology, Kanpur – 208016, India.

Engineers now-a-days utilize a mathematical model to represent a physical (practical) system. Through modelling one can obtain and evaluate information concerning the system's responses to various inputs or stimuli and to predict its behaviour under a given set of conditions. The objective of mathematical modelling is therefore, to develop a simple representation of a complex physical system to study the same easily and conveniently. Modelling is often necessary in the present sophisticated design and analysis procedures, for it is the only way Geotechnical Engineers can analyze a complex physical system at a fraction of the cost of physical or any other type of modelling.

### **Modelling Philosophy**

Before initiating any modelling, the goal of the exercise must be identified first. The requirement of the project or the problem will usually define the goals to be achieved. Simple analytical models are generally sufficient for the first level of understanding. Many of them incorporate very few parameters and do not require a large amount of time for solution or for getting the results. However, all modelling exercises require a proper physical visualization and an understanding of the problem and of the basis under which the solution is being attempted. In particular, the assumptions being made have to be kept in mind, so that the results are not extrapolated beyond the regions for which they are valid. The second level of modelling is usually carried by analytical and/or numerical modelling based on many more conditions, e.g. geometry of the problem, material non-linearities, yield or failure criteria, stress path effects, coupling of time and deformation problems, optimization, probabilistic or stochastic methods, reliability analysis, etc. These second level models may range from a relatively simple one dimensional to more complex three dimensional numerical models. For the latter, many sophisticated methods and software are readily available. Site specific conditions and requirements are easily incorporated in the modelling process.

The commonly utilized models in geotechnical engineering are :

1. Analogue,
2. Centrifuge,
3. Mathematical/Numerical, and
4. Physical.

Amongst these, mathematical/numerical models or modelling has become very common because of the rapid development and decreased cost of digital computers. Data preparation, manipulation, graphical output, etc. have become comparatively easy with the aid of the high speed digital computers already available with the engineering community. A large number of computer codes are readily available. Alternately, it is not very difficult to write problem specific software to conduct numerical experimentation.

## Modelling Process

The modelling process can be visualized as representation of a physical entity, a phenomenon or a process, whose components can vary from a single one to an assemblage of parts and whose characteristic(s) can vary from simple concept to a complex combination of a variety of ideas. The process of building a model or modelling involves identification of the principal features of the actual (real) phenomenon or process in terms of the governing principles or the laws and representing them in the form of a set of relations. The relations are assembled in to one or more number of governing equations which model the response of the physical system or a process to one or more inputs. The steps involved in the modelling process are :

1. Select a problem/system of interest.
2. Postulate the principal characteristic(s) of the problem or system. Idealize and/or simplify the system – modelling of the system.
3. Apply principles of mechanics, viz., Newton's laws, stress-strain relations, strength criterion, effective stress principle, Darcy's law, continuity condition, compatibility condition, stress history, etc., and deduce the response of the model.
4. Compare the predictions with the measured values from carefully conducted *in situ* or laboratory tests.
5. If the agreement between the two is not good, go to step 2, re-examine the postulates and repeat steps 2 to 5.

## Advantages of Modelling

1. It forces one to make explicit assumptions. However, many models exist which make implicit assumptions which are difficult to identify. Some times, these assumptions lead to misunderstanding.
2. Modelling emphasizes the generality of simple decision rules. It should however be borne in mind that this emphasizing may fool one in to thinking that the simple solution is the actual or real behaviour.
3. The most important advantage of modelling is its ability to make precise predictions. it is the precision of mathematics which permits us to test our understanding of a real world problem.

## Physical Modelling

Physical modelling is the most common form of studying the geotechnical problems. Almost all of us at some time or other would have resorted to this technique to investigate the topic of interest. Presently, a large number of studies are still being carried out to understand the mechanisms controlling soil behaviour. However, there are many limitations in physical modelling especially with respect to Geotechnical Engineering problems. In

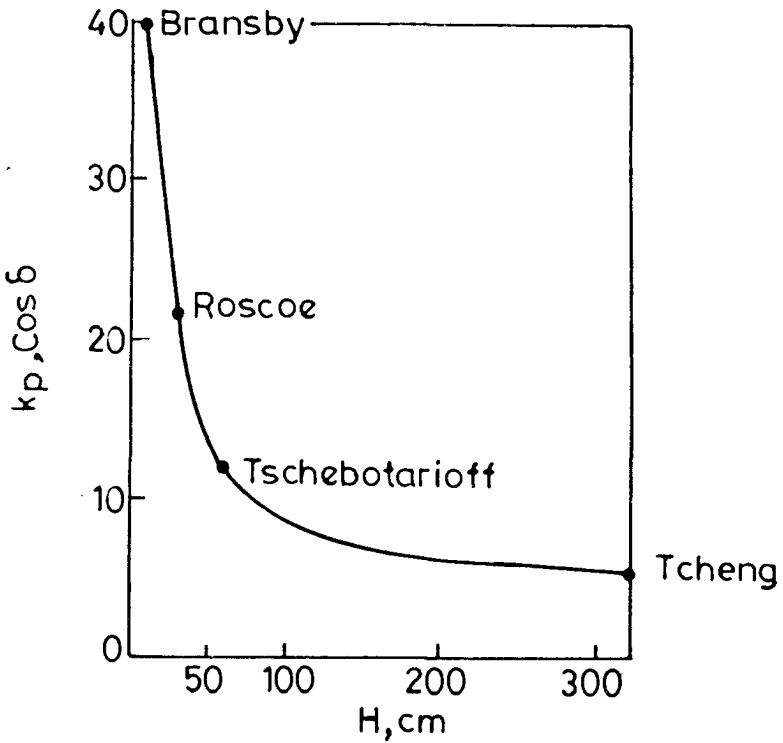


FIGURE 1 : Effect of Height of Wall on  $K_p$  (after Kerisel, 1972)

particular, the scale effect is the most serious one. The stresses operating in a model are a fraction of those in a prototype and the behaviour of the soil is vastly different in the two situations. While the results from the model studies are qualitatively very useful, they can not be extrapolated to real situation.

Kerisel (1972) in his classic lecture discussed the anomalies arising from physical modelling of geotechnical problems. In particular, the coefficient of passive lateral pressure,  $K_p$ , has been shown to decrease (Fig. 1) with the height of the wall in model test.  $K_p$  decreases from about 40.0 to about 6.0 as the wall height increases from 0.1m to 3.0m respectively for the case of dense sands and translating walls. The primary cause for the scale effect, are the low stresses due to gravity and small displacements in the test procedure. The secondary causes are the side wall friction, cohesion, confining stresses, etc. In small sized models, the stresses due to self weight are small, the Mohr-Coulomb envelop markedly non-linear and the displacements relatively small compared to the large sized tests. Kerisel (1972) attempts to explain the discrepancies in the coefficients of passive

pressure through an appropriate choice of angle of shearing resistance between the peak and the residual values.

### Rheological/Visco-Elastic Modelling

The two primary causes for the time lag in the settlement of saturated fine grained soils have been identified as due to hydrodynamic and viscous effects. The former arises due to the low permeability of these soils while the latter is a manifestation of the creep of the soil fabric under constant effective stresses. The classic one-dimensional theory of consolidation of Terzaghi is represented by a simple Kelvin (rheological) model (Fig. 2) consisting of a spring for the deformation response of the soil skeleton in parallel with a dashpot for the dissipation of excess pore water pressure. The creep or the secondary compression phenomenon is then incorporated in the advanced theories of consolidation by improving or modifying the soil skeletal response with time. The mechanical analogue (Gibson and Lo, 1961) for the Taylor-Merchant theory of secondary compression (the rate of secondary compression is proportional to the amount of residual secondary compression) consists of a linear spring in series with a Kelvin body (Fig. 3a). Barden (1965) models for the secondary compression behaviour of soil as a Kelvin body (Fig. 3b) with the dashpot having a non-linear response. Schiffman et al. (1964) develop a series of visco-elastic models to represent the stress-strain-time relationships of soils especially in the secondary compression stage. Starting from the simple spring analogy for the effective stress-strain relation of the soil, more general two, three and five parameter models couple the volumetric and the deviatoric components of the responses.

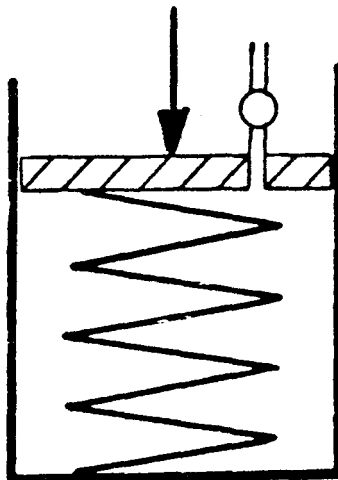


FIGURE 2 : Spring-Dashpot Analogy for One-Dimensional Consolidation

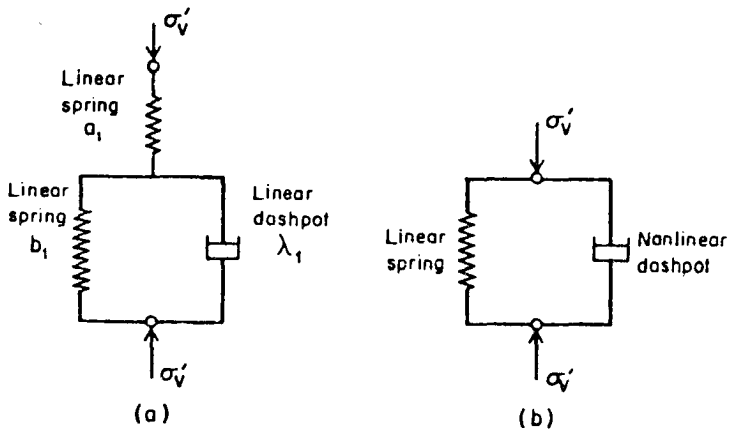


FIGURE 3 : Mechanical Analogy for Secondary Compression  
(a) Gibson and Lo, (b) Barden Models

## Recent Modelling Approaches

Basudhar et al. (1979) have developed a new and versatile approach to study problems of stability of foundations, retaining walls and soil structures combining the discretisation of finite element method with the powerful non-linear programming method of optimization. It has become possible to obtain lower bound solutions which are very close to the upper bound values and thus get an exact result. Catastrophe theory is applied to model landslides (Miao and Ai, 1988). A characteristic relation is developed modelling the landslide as a cuspid catastrophe by means of which the quick landslide can be differentiated from the slow one. In addition, a fundamental formula for the prediction of landslides is deduced through the random process analysis. The formula offers a theoretical basis for the Saito's (1965) method for the prediction of time to failure of a slope. One of the most recent and elaborate modelling exercise has been carried out by El-Fadel et al. (1996) who model the biochemical and physical processes in landfills. The model incorporates biokinetic equations describing the dynamics of the microbial landfill ecosystem into multi-component (methane, carbon-di-oxide and nitrogen) time dependent gas and heat generation and transport models. The model can be used to simulate the gas production, migration and emission at a landfill site and assess the parameters that control biological, physical and chemical processes in a landfill system. The other approaches which have great potential in Geotechnical Engineering are neural networks, fuzzy modelling and fractals.

## Numerical Modelling

In Geotechnical/Ground Engineering, the basic laws or principles governing

the behaviour of soils, foundations, earth structures, etc., can be identified as :

- I Mechanics of Deformable Solids
  - a. Equilibrium Relations;
  - b. Compatibility of Deformations;
  - c. (i) (Elastic/Plastic/Viscous) Stress-Strain Relationships; and  
(ii) Failure or Yield Criterion
- II Flow Problems (Fluid Mechanics)
  - a. Darcy's Law;
  - b. Continuity Condition; and
  - c. Advection/Adsorption/Elasto-kinetics, etc.
- III Dimensionality
  - a. One-Dimensional (Vertical or Radial)
  - b. Two-Dimensional (Plane Strain or Axi-symmetric); and
  - c. Three-Dimensional Problems
- IV Variation of Properties with Position
  - a. Homogeneity;
  - b. Layered Deposits; and
  - c. Non-homogeneity
    - (i) Linear variation with distance
    - (ii) General variation in space
- V Variation of Properties with Direction
  - a. Isotropic;
  - b. Cross-isotropic; and
  - c. Anisotropic
- VI Geologic History/Memory
  - a. Normally Consolidated;
  - b. Over Consolidated; and
  - c. Under Consolidated
- VII Coupled Volumetric and Shear Deformations
  - a. Dilatant; and
  - b. Contractive
- VIII Porous Medium
  - a. Saturated Soil - Effective Stress Principle; and
  - b. Partly Saturated Soil - Pore Pressure and Suction
- IX Physico-Chemical Phenomena
  - a. Expansion;
  - b. Shrinkage;
  - c. Collapse; and
  - d. Cementation
- X Stress Path Effects

Table 1 summarizes the concept invoked in some of the typical problems encountered in geotechnical/ground engineering. It should be noted that the principle of effective stress is implicit in most of the problems and hence is not stated explicitly in the concept listed below.

**Table 1 : Typical Geotechnical Problems and Concepts Involved**

No.	Problem	Concept(s)
<b>BASIC PROBLEMS</b>		
1.	Stability (Bearing Capacity, Earth Pressures, Slope Stability, etc.)	Equilibrium Equations; Strength or Failure Criterion; Plane Strain
2.	Seepage	Two/Three Dimensional Darcy's law; Continuity Condition
3.	Settlement Analysis	One/Two/Three Dimensional Stress-Strain Relations; Equilibrium Equations; Stress History, Stress Path
4.	Foundation-Soil Interactions	Equilibrium Equations; Stress-Strain Relations; Compatibility (Elastic/Elasto-plastic, Tensionless, etc.)
5.	Reinforced Foundation Beds	Equilibrium Equations; Stress-Strain Relations; Interface Shear Resistance; Compatibility, etc.
<b>COUPLED FLOW, DEFORMATION AND STABILITY PROBLEMS</b>		
6.	Consolidation	One/Two/Three Dimensional Darcy's law; Continuity Condition; Stress-Strain Relations; Equilibrium Equations; etc.
7.	Time Dependent Stability	Equilibrium Equations; Failure Criterion; Darcy's law; ; Stress Path, etc.
8.	Stone Columns/Granular Piles	Equilibrium Equations; Constitutive Relations; Compatibility; Darcy's law; Continuity Condition; Failure/Yield Criterion; Dilatancy, etc.

## Modelling Strength of Soils

The shear strength of soil increases with the effective normal stress, and therefore, cannot be generally described by one parameter failure models of Tresca (Fig. 4a) or von Mises (Fig. 4b) except for the case of undrained behaviour of saturated soils when the analysis is performed in terms of total stresses. The one-parameter model of Lade and Duncan (1975) (Fig. 4c) is appropriate for cohesionless soils. The Mohr-Coulomb criterion (Fig. 5c)  $\tau = c' + \sigma' \cdot \tan \phi'$  is the best known failure model for soils, where  $\tau$  and  $\sigma'$  are the shear and normal stresses on the failure plane respectively, and  $c'$  and  $\phi'$  are the cohesion and angle of shearing resistance respectively of the soil. However, it is not mathematically convenient in three dimensional application due to the presence of corners or singularities. The two-parameter

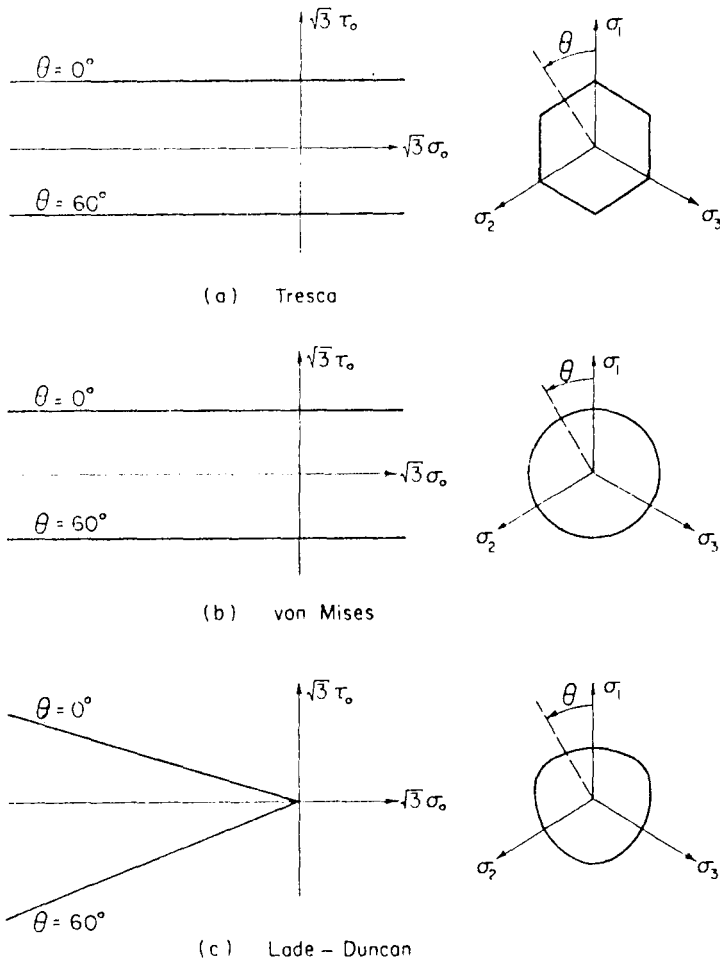
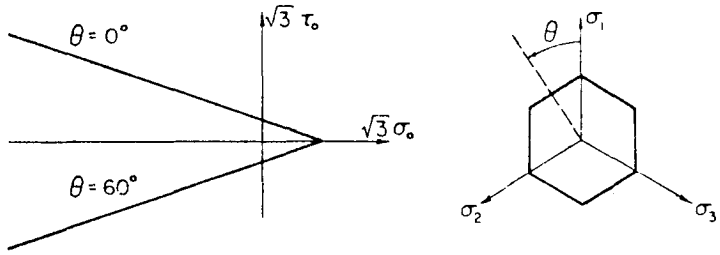


**FIGURE 4 : One-Parameter Failure Models**

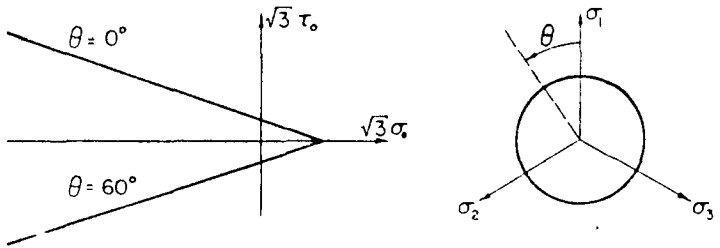
failure model of Lade (1977) has been found adequate for a wide range of stresses for both sands and normally consolidated fine grained soils. The advantages and limitations of the various strength models are listed in Table 2 (Chen and Baladi, 1985).

### Modelling Foundation – Soil Interactions

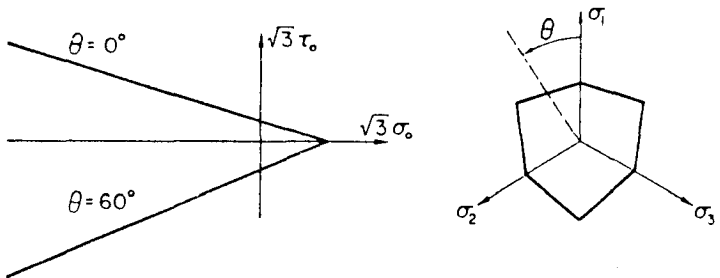
For the prediction of the overall response of a foundation resting on or in soil or ground, a number of simple (one, two or three parameter) models have been proposed and widely used. A major limitation of this approach is that while the gross response of the system can be predicted relatively easily



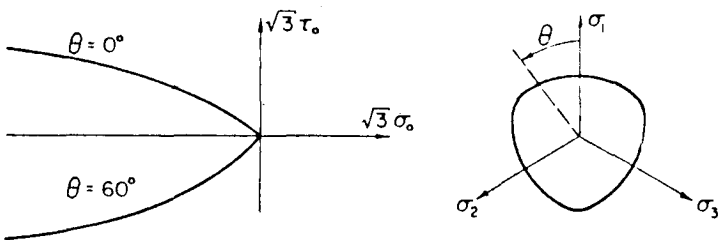
(a) Extended Tresco



(b) Extended von Mises (Drucker - Prager)



(c) Mohr - Coulomb



(d) Lade

FIGURE 5 : Two-Parameter Failure Models

**Table 2 : Advantages and Limitations of Strength Models  
(after Chen and Baladi, 1985)**

Model	Advantages	Limitations
<b>ONE PARAMETER MODELS</b>		
1. von Mises	Simple and smooth	Only for undrained saturated soils (total stress)
2. Tresca	Simple	Only for undrained saturated soils (total stress), Corners
3. Lade-Duncan	Simple, effect of intermediate principal stress, smooth	Only for cohesionless soils
<b>TWO PARAMETER MODELS</b>		
1. Mohr-Coulomb	Simple, validity well established for many soils	Corners, Neglects the effect of intermediate principal stress
2. Drucker-Prager	Simple, smooth, can match Mohr-Coulomb with proper choice of constants	Circular deviatoric trace which contradicts experiments for cohesionless soils
3. Lade's Model	Simple, smooth, wider range of pressures than the other criteria	Only for cohesionless soils

and in simple terms, the local variations of stresses, strains or displacements can not be found out. for such detailed analysis, the Finite or Boundary Element Methods are the preferred choices. The mechanical models currently available are shown in Fig. 6 and are presented below :

**One Parameter Models or Model Elements**

*Winkler Model*

One of the basic characteristics of soil is its compressibility. Conventionally, a linear void ratio - effective stress or a linear void ratio - log effective stress relation is defined to represent the response of a soil element to applied stress. That is

$$\Delta e = a_v \Delta \sigma = C_c \Delta (\log \sigma) \tag{1}$$

where,  $e$  = void ratio,  
 $\sigma'$  = effective stress, and  
 $a_v$  and  $C_c$  = constants of proportionality which characterize the element soil behaviour.

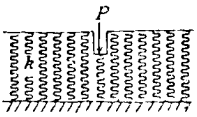
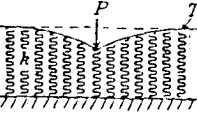
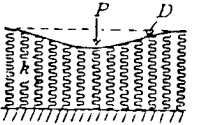
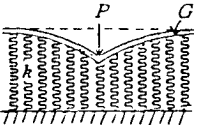
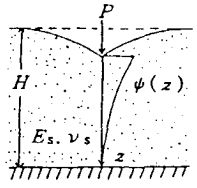
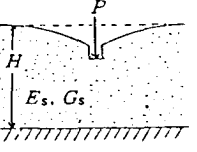
Model of Soil		Mechanical Model and Deflection Curve of the Surface	
One-Parameter Model	Winkler Model	 $y = \frac{P}{k} \delta(x)$ $p = k y$	$\delta(x) : \text{Dirac's Delta Function}$
	Filonenko-Borodich Model	 $y = \frac{P\gamma}{2k} e^{-\gamma x }$ $p = k y - T y''$	$\gamma = \sqrt{k/T}$ $T : \text{Tensile Stress}$
Two-Parameter Model	Hetényi Model	 $y = \frac{P\beta}{2k} e^{-\beta x } (\cos \beta x  + \sin \beta x )$ $p = k y + D y^{(4)}$	$\beta = \sqrt{k/4D}$ $D : \text{Flexural Rigidity}$
	Pasternak Model	 $y = \frac{P\gamma}{2k} e^{-\gamma x }$ $p = k y - G y''$	$\gamma = \sqrt{k/G}$ $G : \text{Shear Rigidity}$
	Vlasov Model	 $y = \frac{P\gamma}{2k} e^{-\gamma x }$ $\gamma = \sqrt{k/2t}$ $k = \frac{E_s(1-\nu_s)}{(1+\nu_s)(1-2\nu_s)} \int_0^H \left(\frac{d\psi}{dz}\right)^2 dz$ $2t = \frac{E_s}{2(1+\nu_s)} \int_0^H \psi^2 dz$ $p = k y - 2t y''$	
	Reissner Model	 $y = \frac{1}{4} \frac{P}{k} \delta(x) + \frac{3}{4} \frac{P\gamma}{2k} e^{-\gamma x }$ $p = \frac{G}{4k} p'' = k y - G y''$	$\gamma = \sqrt{k/G}$ $k = E_s/H$ $G = G_s H/3$

FIGURE 6 : Mechanical Models for Foundation-Soil Response

For representing the response of a medium to applied loads, Winkler (1867) assumed that the deformation,  $w$ , at any point on the surface of the subgrade (soil) is directly proportional to the contact stress,  $p$ , at that point and independent of the contact stress at other point (Fig. 6a). The displacement,  $w$ , beneath the applied load,  $P$  or stress,  $p$ , is related as :

$$P = k \cdot w \quad \text{or} \quad p = k_s \cdot w \tag{2}$$

where,  $k$  is similar to a spring constant and  $k_s$  is the coefficient of subgrade reaction. A major limitation of the Winkler model is that points outside the loaded area do not experience any deformation.

**Shear Layer**

In addition to compressibility, soils deform in shear. A classic example is a granular layer which is relatively incompressible but deforms (Fig. 7) by the mobilization of shear deformations. The shear layer is implicitly included in the Pasternak model to be described in the subsequent section. the relation between displacement,  $w$ , and shear stress,  $\tau_{zx}$ , is expressed as

$$\tau_{zx} = G_s \gamma_{zx} = G_s \frac{dw}{dx} \tag{3}$$

where,  $\gamma_{zx}$  = shear strain, and  
 $G_s$  = shear modulus of the soil

However, Randolph and Worth (1978) and Scott (1981) have used it in

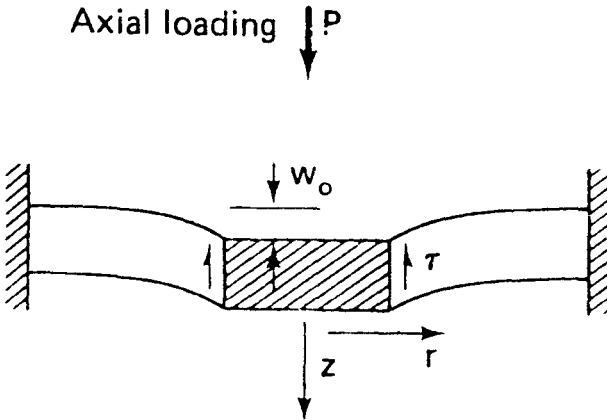


FIGURE 7 : Shear Layer Concept

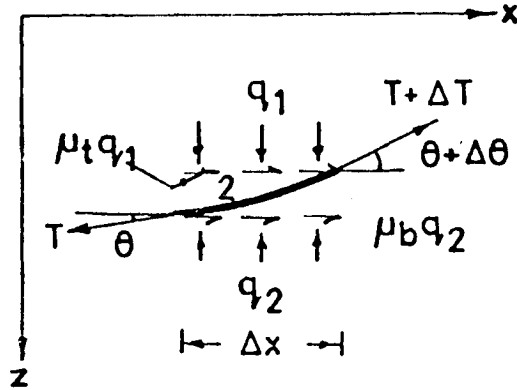


FIGURE 8 : Rough Membrane

isolation for modelling response of piles in soil while Madhav and Poorooshab (1987) model a stiff granular fill as a shear layer. The shear stress at the pile-soil interface is related to the displacement of the pile as

$$\tau_{rz} = k_r \cdot w \quad (4)$$

where,  $k_r = G_s/a \cdot \ln(b/a)$   
 $a =$  radii of the pile, and  
 $b =$  azone of influence of pile.

### *Rough Membrane*

A smooth membrane is incorporated in the Filonenko-Borodich model (discussed in the next section) to provide continuity of deformations. However, the interactions between a reinforcement strip or sheet and soil can be simulated by a rough membrane (Fig. 8) (Madhav and Poorooshab, 1988) whose governing equations are :

$$q_t = q_b - T \cos \theta \frac{d^2 w}{dx^2} \quad (5)$$

$$\frac{dT}{dx} = -q_t (\mu_t \sec \theta + \sin \theta) - q_b (\mu_b \sec \theta + \sin \theta) \quad (6)$$

where,  $q_1$  and  $q_2 =$  stresses,  
 $\mu_t$  and  $\mu_b =$  coefficients of frictional resistances between the reinforcement and the soil on the top and the bottom surfaces respectively, and  
 $\theta =$  slope of the rough membrane.

It is interesting to note that while deriving the governing equations for most of the mode; elements and models, satisfaction of only the vertical force equilibrium equation is adequate, while for the rough element horizontal force equilibrium also needs to be satisfied, as the membrane action is possible only if the latter deforms and generates frictional resistances on its surfaces.

## Two Parameter Models

### *Filonenko-Borodich Model*

A smooth thin membrane with uniform tension,  $T$ , (Fig. 6b) is stretched over a bed of individual springs to achieve continuity of deformations (Filonenko-Borodich, 1940). The governing equation for this model can be derived as :

$$p = k_s \cdot w - T \frac{d^2 w}{d x^2} \quad (7)$$

where  $T$  is the tension in the membrane.

### *Pasternak Model*

A shear layer of unit thickness (Fig. 6d) is combined (Pasternak, 1954) with Winkler springs to combine both compressibility and shear stiffness of the soil or the subgrade and to model continuity of soil deformations on the surface. The shear interaction between the Winkler spring is characterized by the shear stiffness,  $G_p$  ( $= G_s H$ ). The governing equation can be derived as

$$p = k_s \cdot w - G_s H \frac{d^2 w}{d x^2} \quad (8)$$

where  $G_s H$  is the product of the shear stiffness and the thickness of the layer and represents the overall stiffness of the layer. This model is easily conceivable for Geotechnical applications as soils have compressibility and deform in shear. Poorooshasb et al. (1985) extend the Pasternak concept using an analytic approach taking into account the material non-linearity and body forces. The model deals with both failure as well as pre-failure stages of loading.

### *Hetenyi Model*

In his classic book, Hetenyi (1946) proposes incorporating a beam (Fig. 6c) on top of Winkler springs to account for the continuity of

deformations of the subgrade soil. The governing equation becomes :

$$p = k_s \cdot w - E_b I_b \frac{d^4 w}{dx^4} \quad (9)$$

where,  $E_b I_b$  is the flexural stiffness of the beam.

### *Vlasov Model*

The model (Fig. 6e) of soil response proposed by Vlasov (1949) is derived by introducing displacement constraints that simplify the basic equations of linear theory of elasticity for an isotropic continuum and using the variational approach. The state of strain in the subgrade is assumed to be such that the horizontal displacements are zero and the vertical displacements can be expressed as :

$$w(x, z) = w(x) \cdot h(z) \quad (10)$$

where the function  $h(z)$  prescribes the variation of displacements with depth,  $z$ , from the surface. Vlasov and Leontev (1966) propose linear and exponential variations for thin and thick deposits, as

$$\begin{aligned} h(z) &= (1 - \eta), \text{ and} \\ h(z) &= \sinh[\gamma(H - z)/L] / \sinh[\gamma H/L] \end{aligned} \quad (11)$$

where,  $\eta = z/H$   
 $\gamma$  and  $L = \text{constants.}$

The governing equation for the Vlasov model is then derived as :

$$p = k w - 2t \frac{d^2 w}{dx^2} \quad (12)$$

where,  $k = E_0/H(1 - \nu_0^2)$ , and  
 $t = E_0 H/12(1 + \nu_0)$

with,  $E_0 = E_s/(1 - \nu_0^2)$ , and  
 $\nu_0 = \nu_s/(1 - \nu_s)$

for linear variation of displacements with depth. Vlasov model is very similar and almost identical to the Pasternak model and with the additional advantage that the parameter,  $k$  and  $t$  are derived from the elastic deformation parameters

of the subgrade. Kameswara Rao et al. (1971) extend the Vlasov model concept to problems in three dimensions.

### *Elasto-plastic Winkler Model*

The settlement/displacement – stress response from a plate load test is often non-linear. A simple approximation to the actual curve is (Madhav et al., 1971) :

$$q = k_s \cdot w \quad \text{for } w < w_0 \quad \text{or } q < q_{\max}, \quad \text{and} \quad (13)$$

$$q = q_{\max} \quad \text{for } w > w_0 \quad (14)$$

where  $q_{\max}$  is the ultimate bearing capacity of the soil which is presumed to be attained at a settlement of  $w_0$ .

### *Non-linear Winkler Model*

Analyzing data from a number of plate load tests, Chandra et al. (1983) postulate a non-linear stress vs. settlement relationship to represent the subgrade response as :

$$p = k_{s1}w - k_{s3}w^3 \quad (15)$$

where  $k_{s1}$  and  $k_{s3}$  are the two foundation constants. The linear representation valid for small ranges of stresses, is reduced from this general expression with  $k_{s3} = 0$ .

### *Reissner Model*

Reissner (1958) also proposed a model (Fig. 6f) introducing constraints on displacements and stresses that simplify the basic equation for a linear elastic isotropic continuum. The in-plane ( $x$ - $y$  plane) stresses,  $\sigma_x = \sigma_y = \tau_{xy} = 0$  throughout the depth,  $H$ , of the subgrade, and the displacement components,  $u$ ,  $v$  and  $w$  in the  $x$ ,  $y$  and  $z$  directions respectively, satisfy the conditions

$$u = v = w = 0 \quad \text{on } z = H, \quad \text{and}$$

$$u = v = 0 \quad \text{on } z = 0 \quad (16)$$

The response function of the Reissner model is

$$c_1 w - c_2 \frac{d^2 w}{dx^2} = p - \frac{c_2}{4c_1} \frac{d^2 p}{dx^2} \quad (17)$$

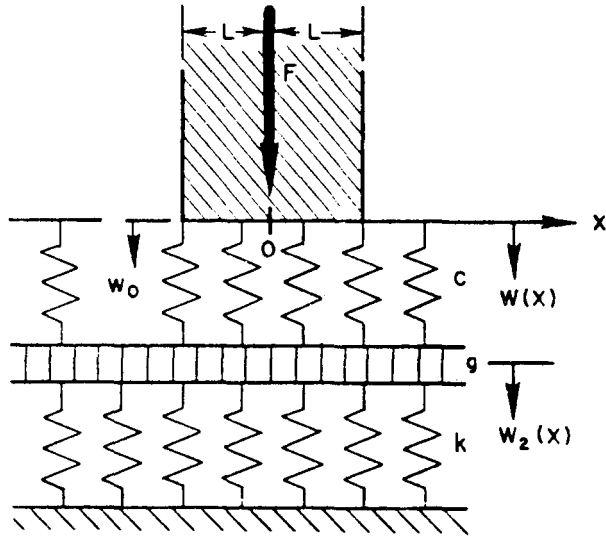


FIGURE 9 : Kerr's Model

where,

$$c_1 = E_s/H$$

$$c_2 = HG_s/3, \text{ and}$$

$E_s$  and  $G_s$  = deformation and shear moduli of the subgrade.

### *Kerr's Model*

As a generalization of Pasternak concept, Kerr (1964) proposed a three parameter foundation model (Fig. 9) which consists of two layers of elastic springs interconnected by an elastic shear layer. The governing equation for this model is derived as :

$$(1 + k_s/c)p - (GH/c)\frac{d^2p}{dx^2} = k_s w - GH\frac{d^2w}{dx^2} \quad (18)$$

where  $c$  and  $k_s$  are the spring constants of upper and lower layer respectively and  $GH$  is the shear stiffness of the shear layer. The advantages of Kerr's model (Kerr, 1965) are :

- (i) the contact pressure response does not include concentrated reactions as in Pasternak model;
- (ii) an additional parameter is available for fitting the theoretical model with experimental results; and

- (iii) in the case of a layer of finite thickness, an additional boundary condition on shear layer deflection is available to simulate the restraint of the foundation layer.

To simulate punch shear failure of foundations on loose or highly compressible soils, Rhines (1969) includes a plastic yielding phenomenon (Fig. 10) in the shear layer of Kerr's model.

**Elastic Continuum Model**

Soil mass usually possesses both compressibility and shear stiffness and it is commonly observed that its surface deforms not only immediately beneath the loaded region but also over regions surrounding the loaded area. Soil mass often is idealized as an elastic semi-infinite continuum to account for the above noted behaviour. The basic equations for the continuum are derived from the theory of elasticity and incorporate the equations of equilibrium, the elastic stress-strain relationships and the compatibility conditions. Any typical problem is solved with these equations and appropriate boundary conditions. Boussinesq (1885) was probably the first to solve the problem of a point load acting on the surface of a homogeneous and isotropic continuum. This fundamental solution has been extensively used in Geotechnical Engineering.

**Reinforcement of Ground**

Reinforcement of soft soils for improvement of bearing capacity and reduction of settlements of structures built on them, is becoming common place. Reinforcement in the form of vertical inclusions, i.e., stone columns/granular piles, sand compaction piles, micropiles, jet grouted piles, etc., is preferred in situations wherein the loaded areas are well demarcated as in the

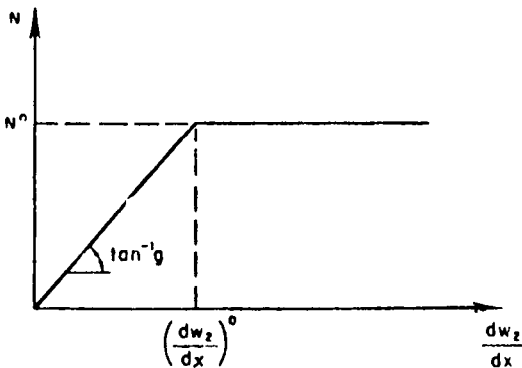


FIGURE 10 : Elastic-Plastic Shear Layer

case of liquid storage tanks, bridge abutments, etc. Horizontal, transverse or lateral reinforcement, in the form of logs, trunks, branches or fascines, have been used from historic times. In recent years, geosynthetics–geotextiles, geogrids, metal strips/grids have replaced the traditional materials in reinforcing the soils for improvement of the bearing capacity and the settlement response of soft soils, especially for unpaved roads and embankments on soft soils, and as semi-rigid pile caps (Miura and Madhav, 1994). The geosynthetics are invariably provided along with a granular fill or bed so that the system may be termed as Geosynthetic Reinforced Foundation Bed (GRFB). The principles and applications of modelling and analysis of geotechnical or ground engineering problems are illustrated in the following sections. In each case, the physics or mechanics of the problem under investigation are identified and the modelling process and analysis developed. Few typical results from numerical experimentation are then presented.

## **Modelling I : Shear Layer Approach**

### ***Granular Piles – Effect of Non-homogeneity***

In most of the available analyses of single and group of granular piles (GP) (Madhav and Nagpure, 1995; Alamgir et al., 1996), the GPs are treated as homogeneous in that their modulus of deformation is constant with depth, while the surrounding soil conditions can be either homogeneous or non-homogeneous. However, since the soil conditions *in situ* are non-homogeneous (both the undrained strength and the modulus of deformation increase with depth even in normally consolidated soils), the GPs installed in them could become inherently non-homogeneous. The compatibility of the GP material increase with depth where the undrained strength is more and larger lateral (confining) stresses are mobilized during the process of installation itself. Where the strength of the *in situ* soil is less and the lateral stresses are smaller, the diameter of the granular pile could be larger, another form (geometric) of non-homogeneity. Figure 11 is a typical illustration which depicts the diameter of GP to be smaller in stiffer and larger in softer strata. GPs tend to enlarge to a larger diameter in softer strata rather than get densified. Therefore, the manifestations of the non-homogeneity of the GP could be an increase in diameter, increase in its unit weight and/or an increase in the modulus of deformation. In this section, a single GP whose modulus of deformation increases with depth is analyzed. Both floating and end bearing GPs are considered as also homogeneous and non-homogeneous *in situ* soil whose stress-deformation response is either linear or hyperbolic.

### ***Formulation***

Figure 12a depicts a single granular pile of diameter,  $d$ , and length,  $L$ , in a soil characterized by its modulus of deformation,  $E_s$ , and Poisson's

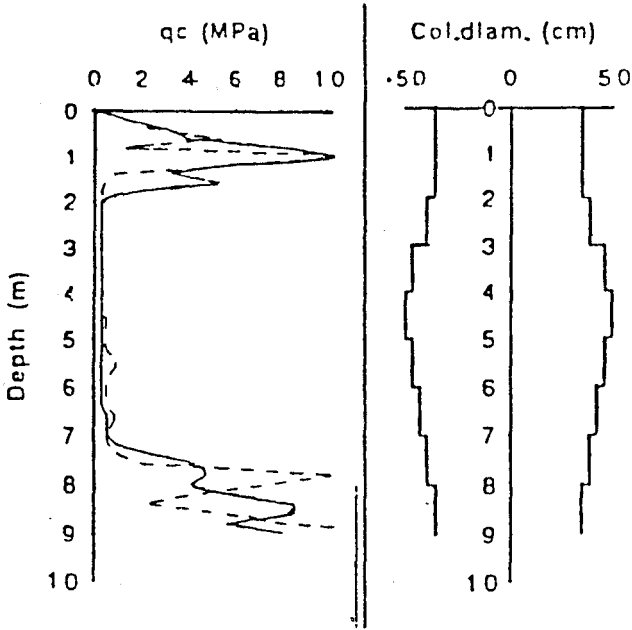


FIGURE 11 : Typical CPT and GP Section  
(after De Cock and D'hoore, 1994)

ration,  $v_s$ . Considering the equilibrium of vertical forces on an element (Fig. 12c), the equilibrium equation reduces to :

$$\frac{d\sigma_z}{dz} = -\frac{4\tau}{d} \tag{19}$$

where,  $\sigma_z$  = vertical shear stress on the element, and  $\tau$  = interfacial shear stress on the element.

Assuming the modulus of deformation,  $E_{gp}(Z)$  of the granular pile to increase linearly (Fig. 12b) with depth,  $z$ , i.e.

$$E_{gp}(Z) = E_{gp0}(1 + \alpha Z) \tag{20}$$

where  $\alpha$  is the rate of increase of the modulus with the normalized depth,  $Z = z/L$ . Assuming the lateral stresses to have negligible effect on vertical strains, the stress-strain relation for the GP is :

$$\sigma_z = E_{gp}(Z)\epsilon_z = -E_{gp0}(1 + \alpha Z)\frac{dw}{dz} \tag{21}$$

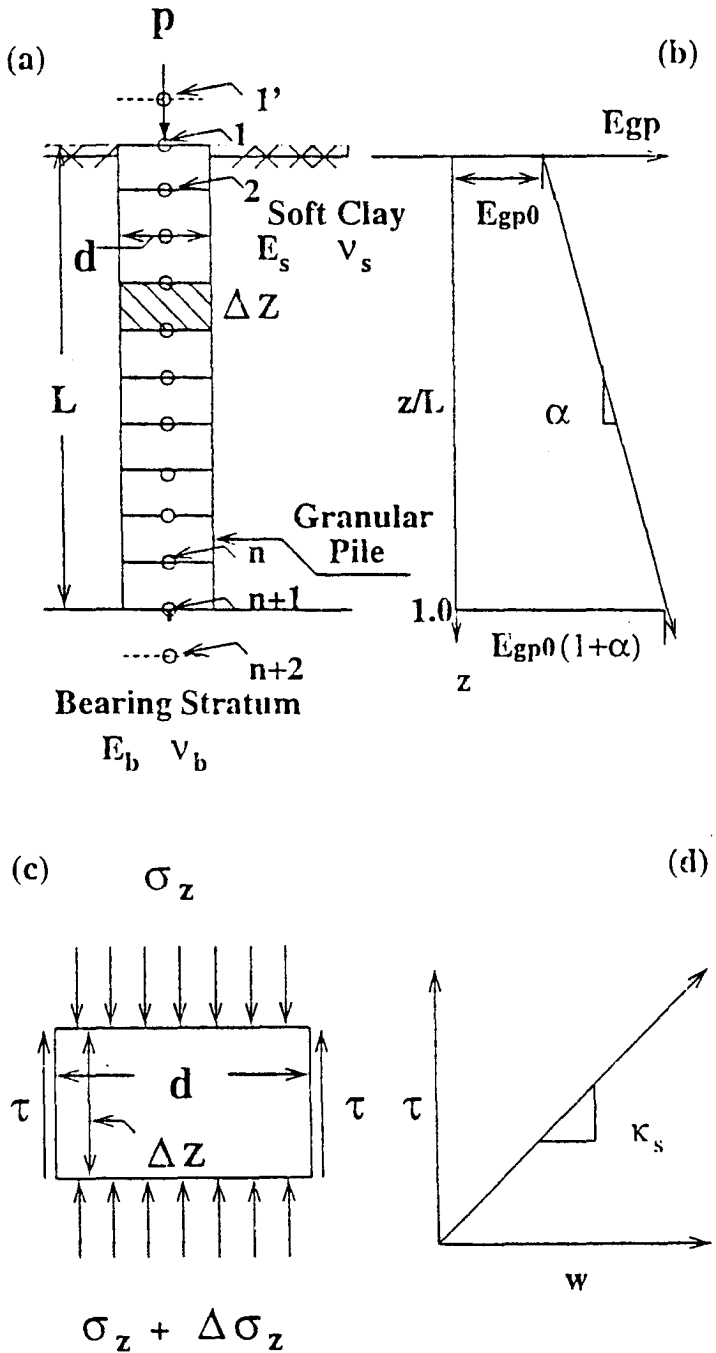


FIGURE 12 : Definition Sketch (a) GP in Soft Soil; (b) Variation of GP Modulus with Depth; (c) Equilibrium of an Element; and (d) Linear Response of Soil

where,  $\varepsilon_z$  = axial strain at depth,  $z$ , and  
 $w$  = displacement

### *Shear Layer Concept*

Following the shear layer model developed by Randolph and Worth (1978) and Scott (1981), the soil response is related to the displacement,  $w$ , as :

$$\tau = k_s \cdot w \quad (22)$$

where  $k_s$  is the shear interaction coefficient for the soil-GP interface. According to Randolph and Worth (1978),

$$k_s = G_s/2d \cdot \ln(2r_m/d) \quad (23)$$

where  $r_m$  is the radius at which the shear stress and/or displacement become zero while Scott (1981) recommends

$$k_s = E_s/(1 + \nu_s)d \cdot \ln(50) \quad (24)$$

Combining Eqns. 22 and 23, one gets

$$(1 + \alpha Z) \frac{d^2 W}{dZ^2} + \alpha \frac{dW}{dZ} - \beta W = 0 \quad (25)$$

where,  $W = w/d$ , and

$$\beta = 4k_s L^2/d E_{gp0}$$

The boundary conditions are :

(i) at the tip of the GP, i.e.  $z = Z = 0$ ,

$$\sigma_z = P/(\pi d^2/4)$$

where,  $P =$  applied load, and

(ii) at the tip or base of the GP, i.e.  $z = 1$  or  $Z = 1$ ,

$w(L) = 0$ , if the GP is resting on a rigid stratum, or

$$w(L) = p_t/k_t$$

where,

$p_t$  = vertical stress at the base of the GP, and

$$k_t = E_b / \left( (1 - \nu_b^2) d \cdot I \right)$$

$E_b$  and  $\nu_b$  = deformation parameters of the base layer, and

$I$  = influence coefficient (Poulos and Davis, 1975).

### *Non-linear Response of Soil*

If the shear stress is related to displacement hyperbolically (Fig. 13), the relation is expressed as :

$$\tau = k_{si} d \cdot w / (1 + \gamma w) \quad (26)$$

where,

$k_{si}$  = slope of the stress-displacement curve at the origin,

$\gamma = k_{si} d / \tau_m$ , and

$\tau$  = maximum shear resistance at the interface.

The normalized form of the governing equation incorporating the hyperbolic response at the interface is :

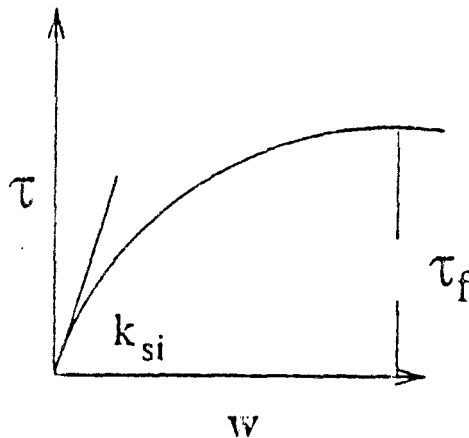


FIGURE 13 : Hyperbolic Stress-Displacement Response of Soil

$$(1 + \alpha Z) \frac{d^2 W}{dZ^2} + \alpha \frac{dW}{dZ} - \frac{\beta W}{(1 + \gamma W)} = 0 \quad (27)$$

When  $\gamma = 0$ , Eqn. 27 reduces to Eqn. 25, the one for linear soil response. For a given applied load, Eqn. 27 has to be solved iteratively as the normalized displacement,  $W$ , appears in the denominator of the third term. It has been found to be tedious and time consuming. As an alternative, an incremental approach is adopted in which the applied load is increased in small increments and for each step, the increments in displacements at all the nodes evaluated. The incremental displacements are summed up to arrive at the displacements of the nodes corresponding to the applied load. Equation 27 in incremental form becomes :

$$(1 + \alpha Z) \frac{d^2 \Delta W}{dZ^2} + \alpha \frac{d \Delta W}{dZ} - \frac{\beta \Delta W}{(1 + \gamma W)^2} = 0 \quad (28)$$

where,  $\Delta W$  = incremental displacement.

The finite difference form of Eqn. 28 is :

$$(1 + \alpha Z_i) \left[ \frac{\Delta W_{i+1} - 2 \Delta W_i + \Delta W_{i-1}}{(\Delta Z)^2} \right] + \alpha \left[ \frac{\Delta W_{i+1} - \Delta W_{i-1}}{2 \Delta W} \right] - \frac{\beta \Delta W_i}{(1 + \gamma W_i)^2} = 0 \quad (29)$$

where  $\Delta Z = 1/n$ . For interior nodes, i.e.,  $I = 2$  to  $n$ .  $DW$  can be solved from

$$\Delta W_i = \frac{\left[ n^2(1 + \alpha Z_i) + \alpha \frac{n}{2} \right] \Delta W_{i-1} + \left[ n^2(1 + \alpha Z_i) - \alpha \frac{n}{2} \right] \Delta W_{i+1}}{\left[ 2 n^2(1 + \alpha Z_i) + \beta / (1 + \gamma W_i)^2 \right]} \quad (30)$$

For displacements at node 1 and  $(n + 1)$  appropriate boundary conditions (Fig. 12a) are applied and Eqn. 30 modified and solved.

### *Numerical Experimentation*

The governing equation, Eqn. 28, is solved in finite difference for (Eqn. 30) and the results are obtained numerically. Firstly the GP is discretized in

to 'n' elements of equal length,  $\Delta L = L/n$ . The accuracy of the results increases with increase in 'n' but further improvement is negligible for  $n > 30$ . Hence  $n = 30$  is adopted in all further work. The results obtained numerically for a homogeneous GP (modulus of deformation constant with depth or  $\alpha = 0$ ), are compared with the exact analytical solutions (Scott, 1981) for a pile bearing on a rigid stratum and a floating pile. The difference between the two sets of results are very small ( $< = 10^{-4}\%$ ), thus validating the numerical analysis and the results. Numerical experimentation is then carried out for the following ranges of parameters :

$$L/d = 2, 5, 10 \text{ and } 100$$

$$K = 5, 10, 25 \text{ 50 and } 100$$

$$\alpha = 0, 0.5, 1.0 \text{ and } 2.0$$

$$\mu_b = 1, 2, 5, 10, 25, 50 \text{ and } 100.$$

The Poisson's ratio of the *in situ* soil is taken as 0.5 (undrained condition) while that of the bearing stratum ( $\mu_b > 1$ ) is 0.3. For a floating GP,  $\mu_b = 1.0$  and  $\nu_b = 0.5$ .

### Results

The variation of the normalized displacement of the GP at its top,  $W_1$ , with normalized depth,  $Z$ , is depicted in Figs. 14 and 15. For a low stiffness ratio,  $K (= E_{gp0}/E_s)$  of the GP, the top and tip settlements (Fig. 14a) are respectively 0.505 and 0.00381. Since the GP is highly compressible, very little load is transmitted to the base and hence the tip settlement is negligibly small. With increasing values of relative GP-soil stiffness,  $K$ , the settlements at the two points tend to become uniform. For  $K = 50$ , the settlements are 0.1268 and 0.0229. The effect of the degree of non-homogeneity,  $\alpha$ , of the GP, on settlements can be seen in Fig. 14b. Settlements of a GP are maximum for a homogenous GP (constant modulus or  $\alpha = 0$ ) but decrease with increasing degree of non-homogeneity ( $\alpha > 1.0$ ). For  $\alpha$  increasing from 0 to 2.0, the top settlement decreases from 0.233 to 0.172, a reduction of 26%. The corresponding reduction in tip settlement is 38%.

The stiffness of the base layer has a very significant effect on the displacements of the GP (Fig. 15a). Both the top and tip displacements decrease with increasing values of the base stiffness ratio,  $\mu_b$ , with the tip displacements decreasing much more than the top ones, as can be expected. The effect of base stiffness for  $\mu_b > 50$ , on GP displacements is negligible, the base behaving almost like a rigid one. The  $L/d$  ratio of the GP has a very significant effect on settlements (Fig. 15b), Smaller  $L/d$  ratio implies not only a shorter GP but also that the bearing stratum is closer to the ground surface. Therefore the GP settlements are smaller

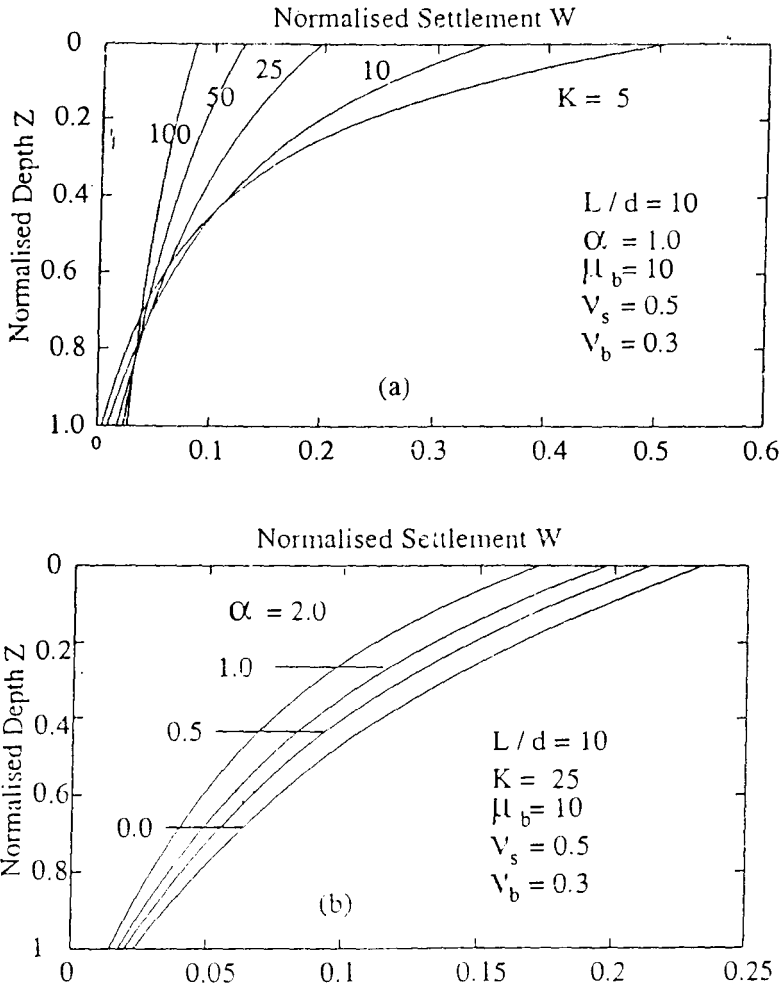


FIGURE 14 : Variations of Normalized Displacements with Depth.  
 - Effect of (a)  $K$ ; and (b)  $\alpha$

for short GP than for longer ones. Interestingly, while the top settlements increase with  $L/d$ , the tip ones decrease since the load transferred to the base is less in the case of longer GP.

The effects of the parameters,  $K$  (relative GP-soil stiffness),  $\alpha$  (degree of non-homogeneity of GP modulus),  $\mu_b$  (relative stiffness of base) and  $L/d$  ratio, on the variation of normalized shear stress ratio ( $\tau/\tau_{avg}$  with  $\tau_{avg} = P/\pi dL$ ) with depth can be seen in Figs. 16 and 17. The variation of shear stress with depth (Fig. 16a) is very similar to that of solid piles (Poulos and Davis, 1980). The stiffer the GP, the more uniform are the shear stresses

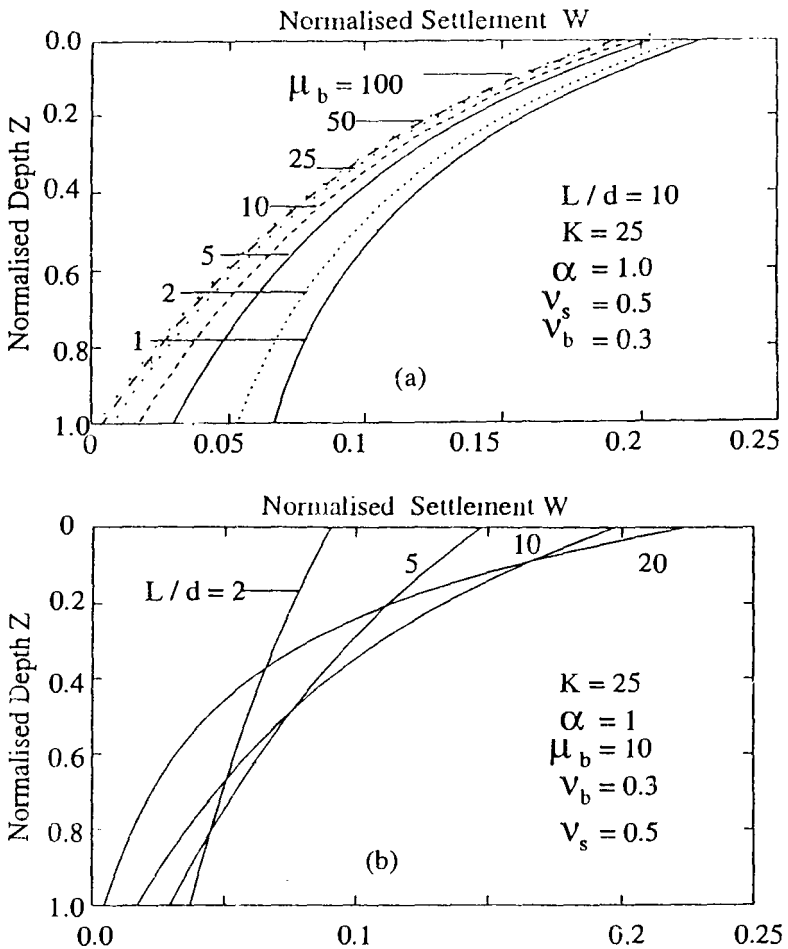


FIGURE 15 : Variations of Normalized Displacements with Depth  
- Effect of (a)  $\mu_b$ ; and (b)  $L/d$

and larger would be the load transferred to the base. The trends in the variations of normalized shear stress (Figs. 16a, 17a and 17b) with depth as effected by the parameters  $K$ ,  $\mu_b$  and  $L/d$ , are very similar to the variations of displacements with these same parameters. However, the effect of the parameter,  $\alpha$ , on the variation of shear stress with depth (Fig. 16b) is somewhat different from the corresponding variations of displacements. The shear stress near the top of the GP increases with increasing values of  $\alpha$ , since a larger value implies a more compressible GP near the top compared to the value of the modulus at the tip. A non-homogeneous GP behaves like a relatively more compressible pile than a homogeneous one.

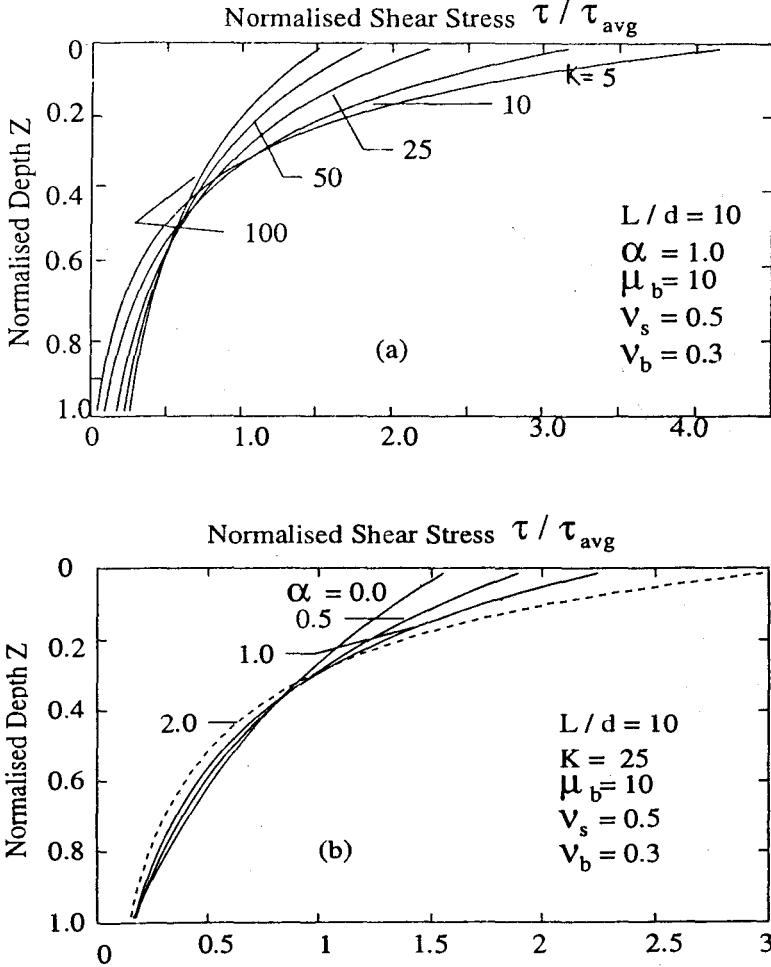
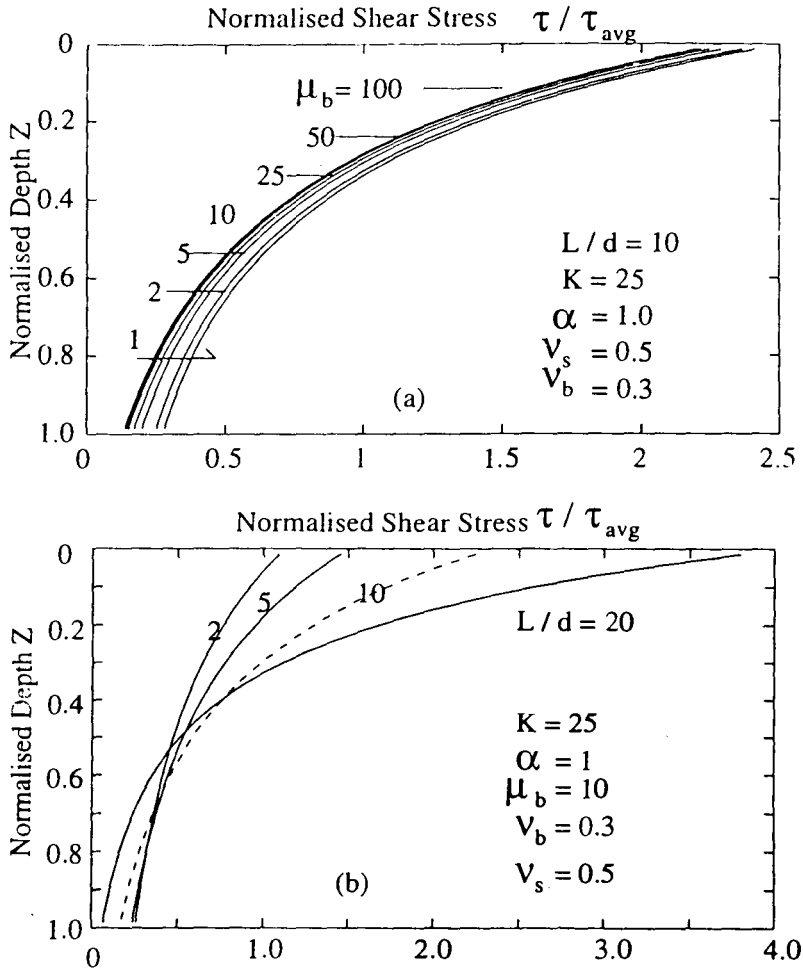


FIGURE 16 : Variations of Normalized Shear Stresses with Depth  
 - Effect of (a)  $K$ ; and (b)  $\alpha$

*Effect of Non-linear Soil Response*

The effect of the non-linearity parameter,  $\gamma (= k_{si} d / \tau_m)$  on the load versus normalized settlement,  $W_1$ , of the GP is depicted in Fig. 18 for  $L/d = 10$ ,  $\alpha = 1.0$  and  $\mu_b = 10.0$ . The parameter,  $\gamma$ , signifies the relative effect of the maximum values of the shear stress at the GP-soil interface. The degree of non-linearity has a very significant effect on the load-settlement curves. The top GP settlements are 0.051, 0.0782, 0.129 and 0.512 at a load of 20 T for  $\gamma$  equal to 0, 20 and 30 respectively. The highly non-linear curves for  $\gamma = 30$  implies the full mobilization of maximum shear resistance near the top of the GP.



**FIGURE 17 : Variations of Normalized Shear Stresses with Depth  
- Effect of (a)  $\mu_b$ ; and (b)  $L/d$**

The variation of normalized shear stress,  $\tau/\tau_m$ , with depth at different applied load levels can be seen in Fig. 19a, for  $L/d = 10$ ,  $K = 25$ ,  $a = 1.0$ ,  $m_b = 10.0$  and  $\gamma = 1.0$ . The shear stresses are more near the top and decreases somewhat with depth. With increasing applied load, the proportions of mobilized shear stresses increase. For the case discussed, the shear stress mobilized is 45% of the maximum. A similar trend of  $\tau/\tau_m$  increasing with  $\gamma$  can be noted in Fig. 19b. The more non-linear the soil response, the higher would be the values of the normalized shear stresses.

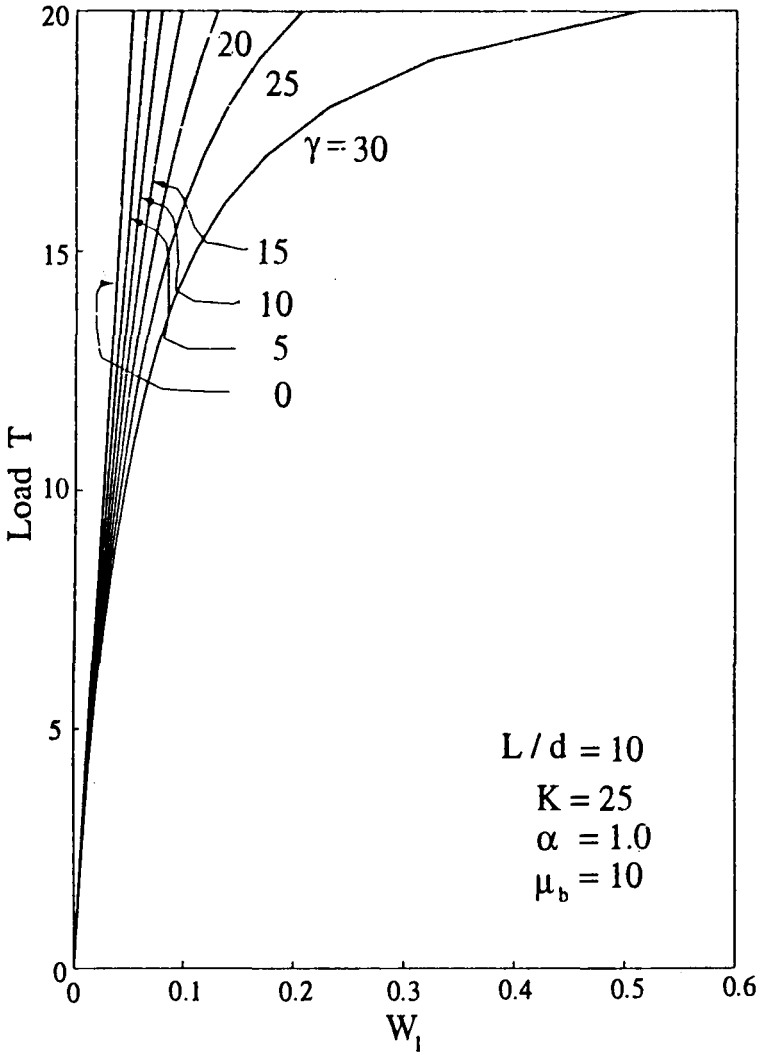


FIGURE 18 : Load vs. Normalized Settlement of GP  
- Effect of  $\gamma$

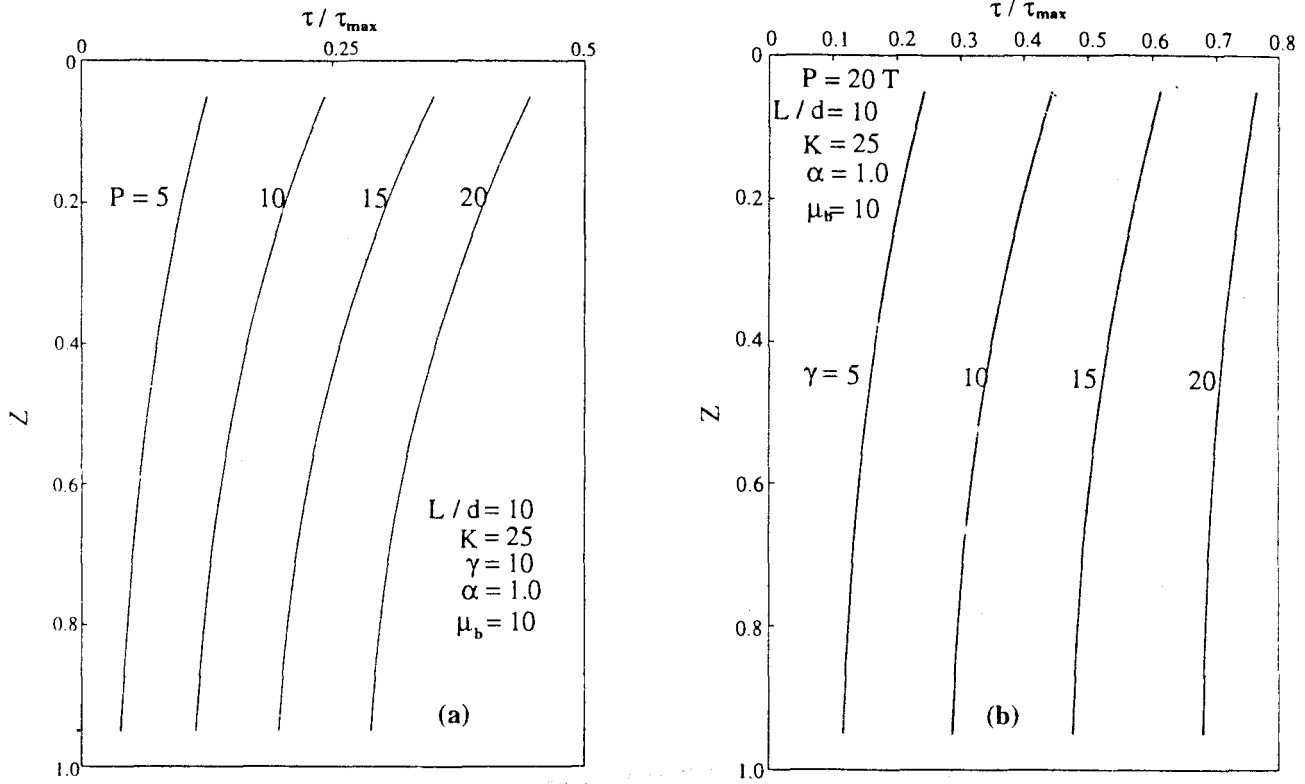


FIGURE 19 : Effect of (a) Load; and (b)  $\gamma$  on  $\tau/\tau_m$

## Modelling II : Bearing Capacity of Reinforced Foundation Beds on Soft Ground

For construction over soft ground, a reinforced granular layer is provided to improve trafficability and provide stability to structure, e.g. embankments, built on the site. In such instances, a geosynthetic reinforcing layer is laid on the soft ground and a granular or earth fill spread over it. The membrane action is generated by the horizontal continuity and the tensile resistance of the geosynthetic under the earth fill and the applied loads. The tensile force produced at the edges is transferred to the soil back by interfacial friction between the soil and the reinforcement or by fixing the latter to anchor piles driven into the ground.

### *Bearing Capacity : Mechanism of Reinforcement*

For the estimation of the load carrying capacity of RFB, different approaches are available. They may be categorized as :

1. Tension/Membrane Effect (Giroud and Noiray, 1981)
2. Lateral Thrust and Shear Interaction Approach (Houlsby et al., 1989; Milligan et al., 1989); and
3. Shear Layer, Confinement and Surcharge Method (Shivashankar et al., 1993)

### *Mechanisms*

The ultimate bearing capacity,  $q_{RFB}$ , can be estimated as the sum of the (i) the bearing capacity of the original ground,  $q_1$ , (ii) the vertical component of tensile force in the reinforcement,  $q_2$ , (iii) the surcharge effect arising from the reinforced bed transferring the stresses to the ground outside the loaded area,  $q_3$ , and (iv) the embedment effect resulting from the settlement of the loaded area and the heave outside,  $q_4$ , as

$$q_{RFB} = q_1 + q_2 + q_3 + q_4 \tag{31}$$

where,

$$q_1 = c_u \cdot N_c$$

$$q_2 = 2 \cdot T \cdot \sin \theta / B$$

$$q_3 = T \cdot N_q / r$$

$$q_4 = \gamma_t \cdot D_f$$

$c_u$  = undrained cohesion of the soft ground,

$N_c$  and  $N_q$  = bearing capacity factors,

$T$  = tensile force in the reinforcement material,

$\theta$  = angle formed by the reinforcement and the horizontal surface at the edge of the load,

$B$  = width of the loaded area,

$r$  = radius of the deformed shape of the ground near the edge of the load when the shape is considered as circular,

$\gamma_t$  = unit weight of the soil, and

$D_f$  = depth of embedment (sum of settlement at the edge and the heave outside).

The force  $T$  and the deformation parameters,  $r$ ,  $\theta$  and  $D_f$  are measured or often extrapolated from laboratory tests.

### *Shear Layer, Confinement and Surcharge Method*

Reinforced granular bed over a soft soil (Fig. 20) increases the bearing capacity of a footing resting on it, in several ways. A punching shear failure mode can be envisaged in which both the footing and the portion of the reinforced granular layer directly beneath the footing act in unison to punch through the soft clay underneath. The granular bed contributes to the shear layer effect. Meyerhof (1974) considers this aspect and proposes a relation for the estimation of the ultimate bearing capacity of a granular layer overlying soft clay.

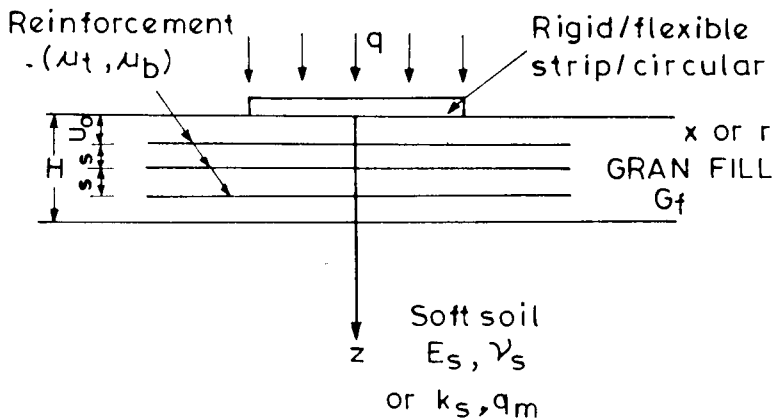


FIGURE 20 : Reinforced Granular Bed over Soft Soil

Madhav and Sharma (1991) consider the contribution of the stress transfer to the soil outside the loaded area and propose an extra component to the bearing capacity due to the additional surcharge effect. For reinforcements longer than the footing width, frictional resistances are mobilized by the reinforcement and the granular material at the interfaces on either side of the footing, and the reinforcement would be subjected to tensile stresses. The tensile stresses provide confinement effect to the block of granular soil below the footing. This in turn, would cause additional shearing resistances to be mobilized along the vertical planes through the edges of the footing. The total shear resistances generated along these vertical planes, due to shear layer and confinement effects, get redistributed as additional exponentially decreasing surcharge stresses onto the lower soft clay layer. This additional surcharge would further increase the bearing capacity of the system. Madhav and Datye (1993) present a theory for the estimation of bearing capacity of a footing with variable surcharge.

Combining all these contributions, the bearing capacity,  $q_u^*$ , of a footing resting on a geosynthetic reinforced granular layer overlying soft clay, can thus be expressed as :

$$q_u^* = c_u N_c + \Delta q_{SL} + \Delta q_{CE} + \Delta q_{SE} \quad (32)$$

where,  $c_u$  = undrained strength of the soft soil,  
 $N_c$  = bearing capacity factor,  
 $\Delta q_{SL}$  = increase in the bearing capacity due to shear layer,  
 $\Delta q_{CE}$  = increase in the confinement, and  
 $\Delta q_{SE}$  = increase in the surcharge.

The surcharge component arises predominately due to the reinforcement which contributes to both the surcharge and confinement effects. In the absence of the reinforcement layer, the confinement effect will be absent and the surcharge effect would be less compared to the case with the reinforcement. Defining the bearing capacity ratio,  $BCR = q_u^*/c_u \cdot N_c$ , one obtains

$$BCR = 1 + \Delta BCR_{SL} + \Delta BCR_{CE} + \Delta BCR_{SE} \quad (33)$$

where  $\Delta BCR_{SL}$  = increments in the bearing capacity ratios due to the shear layer,  
 $\Delta BCR_{CE}$  = increments in confinement, and  
 $\Delta BCR_{SE}$  = increments in surcharge effects.

Shivashankar et al. (1993) have derived the three effects as follows :

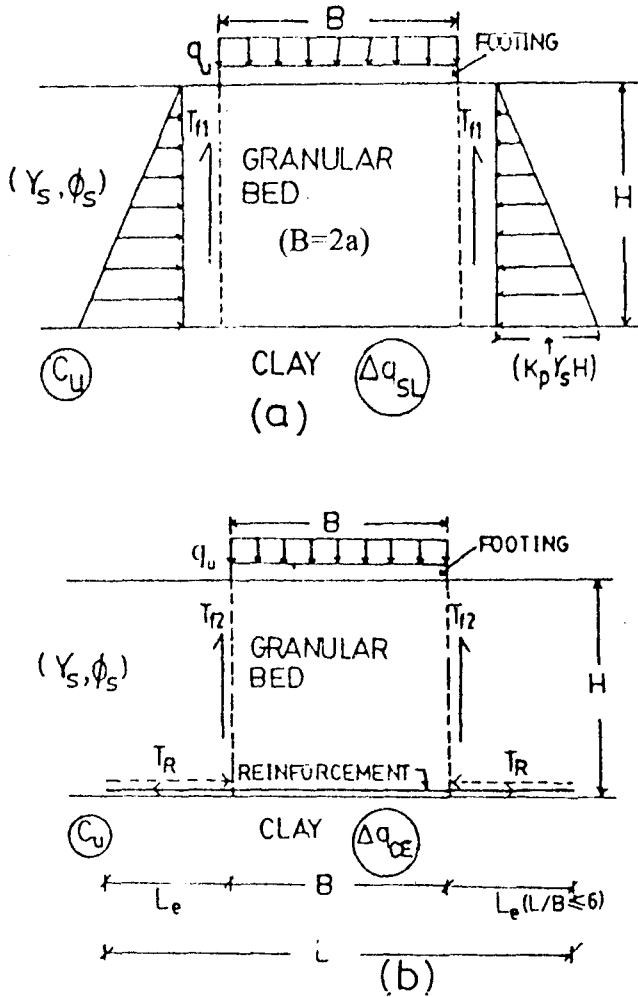


FIGURE 21 : (a) Shear Layer; and (b) Confinement Effects

1. *Shear Layer Effect* : Lateral stresses developed (Fig. 21a) in the granular layer above the reinforcement cause shear stresses,  $T_s$  to be mobilized, when the footing and the associated granular bed punch through the soft clay underneath. The bearing capacity effect due to the shear layer effect expressed in term of  $\Delta BCR_{SL}$ , is

$$\Delta BCR_{SL} = 2 T_f / B c_u N_c \tag{34}$$

where,  $T_f = K_p \gamma_s H^2 (\tan \phi_s)$

- $K_p$  = coefficient of passive earth pressure,
- $H$  = thickness of the granular bed,
- $\gamma_s$  = unit weight of the granular bed,
- $\phi_s$  = angle of shearing resistance of the granular bed, and
- $B$  = width of the footing

2. *Confinement Effect* : The tensile forces mobilized in the reinforcement,  $T_R$ , (Fig. 21b) outside of the loaded area also contribute to the shear stresses. The contribution from the reinforcement to the confinement effect,  $\Delta BCR_{CE}$ , is

$$\Delta BCR_{CE} = 2TR \cdot \tan \phi_s / B c_u N_c \tag{35}$$

3. *Surcharge Effect* : The shear stresses carried by the granular layer and the tensile forces in the reinforcement, are transferred back to the soil as surcharge (Fig. 22). The contribution to the bearing capacity from the surcharge effect,  $\Delta BCR_{SE}$ , is

$$\Delta BCR_{SE} = f(R_q) \tag{36}$$

where,

$$R_q = (q_{s0} + \gamma_s H) / c_u$$

$$q_{s0} = 0.84(\Delta BCR_{SL} + \Delta BCR_{CE})$$

Combining Eqns. 33 through 36, the BCR of the RFB is easily estimated. The predicted BCR values are compared (Fig. 23 and Table 3) with the experimental values compiled from published results. The break-up of the individual contributions of the three effects are shown in Table 3. The proposed method appears to predict well the improvement in bearing capacity of RFB.

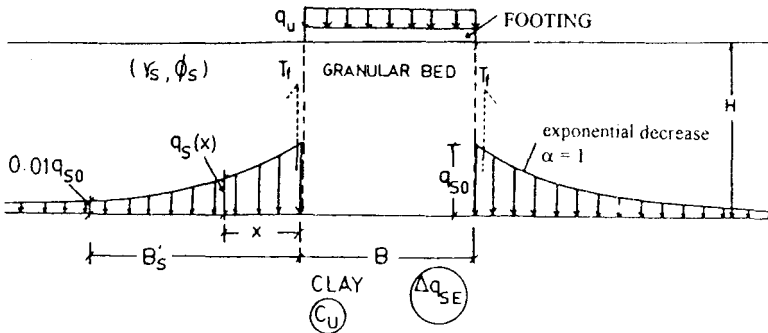


FIGURE 22 : Surcharge Effect

Table 3 Predicted and Measured BCR Values (with break-up of predicted BCR Values)

Authors	$C_u$ T/m <sup>2</sup>	$\phi_u$ degrees	H/a	L/B	BCR		ΔBCR		
					Experimental	Predicted	SL	CE	SE
Love et al. (1986)	0.60	45	1.33	13.33	1.48	1.40	0.11	0.10	0.19
	0.90	45	1.33	13.33	1.60	1.28	0.08	0.06	0.14
	1.40	45	1.33	13.33	1.60	1.19	0.04	0.04	0.10
	0.60	45	2.00	13.33	1.63	1.63	0.26	0.14	0.24
	0.90	45	2.00	13.33	1.78	1.78	0.17	0.10	0.20
	1.40	45	2.00	13.33	1.46	1.46	0.11	0.07	0.15
	0.60	45	2.67	13.33	1.72	1.94	0.45	0.20	0.29
	0.90	45	2.67	13.33	1.9 - 2.67	1.68	0.30	0.13	0.25
	1.40	45	2.67	13.33	1.54	1.48	0.19	0.09	0.20
	Dembicki et al. (1986)	0.55	30	1.00	13.25	1.3 - 1.42	1.24	0.05	0.06
0.55		30	2.00	13.25	1.4 - 1.46	1.54	0.18	0.12	0.24
0.55		30	1.00	5.00	1.04 - 1.1	1.22	0.05	0.05	0.12
0.55		30	2.00	5.00	1.30 - 1.4	1.51	0.18	0.10	0.23
Jarrett (1986)	0.36	37	1.48	18.22	1.80	1.79	0.28	0.24	0.27
	0.36	37	2.96	18.22	2.93	2.94	1.11	0.47	0.36
	0.36	37	4.44	18.22	5.33	4.57	2.51	0.71	0.35
	0.36	37	1.48	0.00	1.27	1.52	0.28	0.00	0.24
	0.36	37	2.96	0.00	2.26	2.45	1.11	0.00	0.34
	0.36	37	4.44	0.00	3.20	3.87	2.52	0.00	0.35
Milligan et al. (1986)	3.30	45	1.00	8.17	1.20	1.22	0.05	0.05	0.12
	3.30	45	1.33	8.17	1.23	1.31	0.08	0.07	0.16

Table 3 contd.

Authors	$C_u$	$\phi_u$	H/a	L/B	BCR		$\Delta$ BCR		
	T/m <sup>2</sup>	degrees			Experimental	Predicted	SL	CE	SE
Yamauchi & Kitamori (1985)	0.30	26	0.67	5.00	1.40	1.45	0.08	0.13	0.24
	0.30	26	0.67	0.00	1.30	1.25	0.08	0.00	0.12
Milligan & Love (1984)	0.60	45	1.33	13.33	1.24 - 1.5	1.39	0.11	0.10	0.18
	1.00	45	1.33	13.33	1.5 - 1.63	1.25	0.07	0.06	0.12
	1.60	45	1.33	13.33	1.6 - 1.75	1.17	0.04	0.04	0.09
	0.06	45	2.00	13.33	1.3 - 1.58	1.64	0.26	0.15	0.23
	1.00	45	2.00	13.33	1.59 - 1.8	1.43	0.15	0.09	0.09
	1.60	45	2.00	13.33	1.3 - 1.45	1.29	0.10	0.06	0.13
	0.60	45	2.67	13.33	1.4 - 1.7	1.94	0.45	0.20	0.29
	1.00	45	2.67	13.33	1.87 - 1.9	1.63	0.27	0.11	0.25
	1.60	45	2.67	13.33	1.52 - 1.8	1.43	0.17	0.07	0.19
Gourc et al. (1982)	0.90	34	1.33	0.00	1.04	1.16	0.06	0.00	0.19
	2.70	34	1.33	0.00	1.07	1.06	0.02	0.00	0.04
	0.90	48	1.33	0.00	1.41	1.37	0.20	0.00	0.17
Present Study	0.30	43	1.00	0.00	1.50	1.53	0.40	0.00	0.13
	0.30	43	1.00	2.00	1.90	1.80	0.40	0.00	0.22

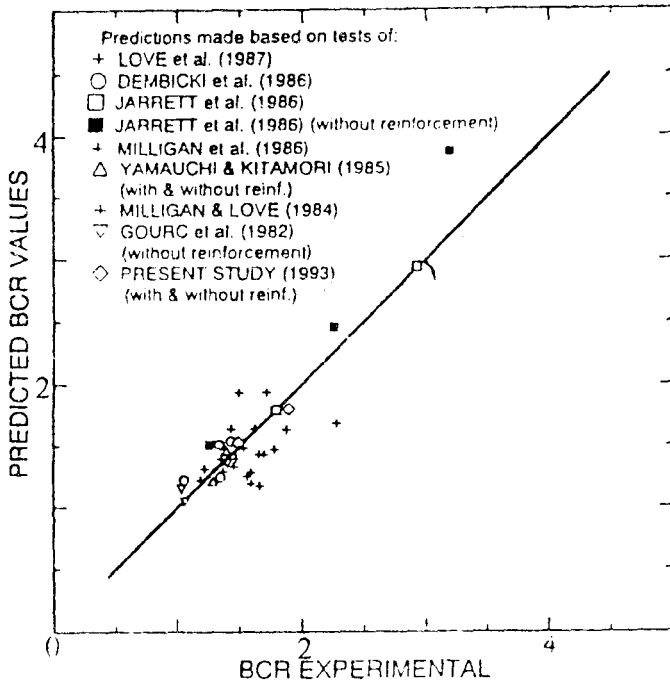


FIGURE 23 : Comparison of Predicted and Measured BCR  
(after Shivashankar et al., 1993)

### Modelling III : Macro/Global Response of RFB on Soft Soil

In the previous section, the modelling of an RFB for the prediction of its ultimate bearing capacity has been presented. In practice, the complete load/stress-settlement response of the RFB is desired. To arrive at its prediction, the different components of RFB (Fig. 24a) and their characteristics have been identified as :

**1. Soft Soil :** Usually, the soft soil extends to a significant depth. It can be modelled as a continuum considering its basic deformation parameters, the undrained modulus,  $E_{su}$ , and the undrained cohesion,  $c_u$ , or as a Winkler medium (Fig. 24b) with the coefficient of subgrade reaction,  $k_s$ , and the net ultimate undrained bearing capacity,  $q_u$  ( $c_u \cdot N_c$ ). The complete stress-settlement relation for the soft soil can be expressed by the hyperbolic relation

$$p = k_s w / (1 + \gamma w) \quad (37)$$

where,  $\gamma = k_s / q_u$ , a non-linear response parameter.

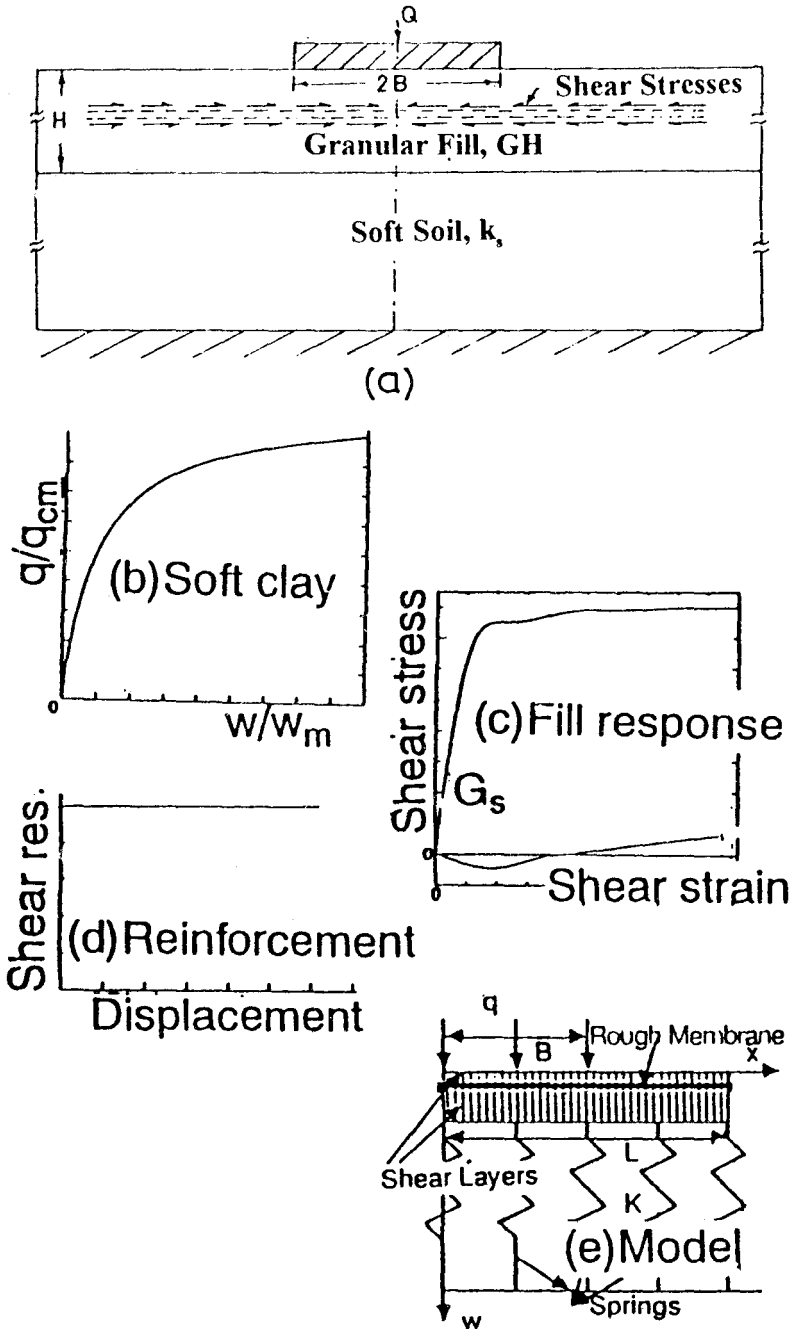


FIGURE 24 : Definition Sketch (a) Reinforced Foundation bed; Responses of (b) Soft Soil; (c) Granular Fill; (d) Reinforcement; and (e) The Model

Thus, the soft clay deposit is modelled as a Winkler foundation with hyperbolic stress-displacement response.

**2. Granular Fill :** The granular fill is relatively incompressible but deforms in shear. Therefore, it is modelled as a shear layer. Since relatively large deformations are possible in case of RFB, the complete shear-stress strain relationship for the granular layer is

$$\tau_{zx} = G\gamma_{zx} / \left(1 + b_s \gamma_{zx}\right) \quad (38)$$

where,  $b_s = G/\tau_m$ , another non-linearity parameter, and  
 $\tau_m = \sigma' \tan \phi'$ , maximum shear resistance of the granular fill.

Following Madhav and Porooshab (1987) the granular fill is modelled as a (Pasternak) shear layer with non-linear response (Fig. 24c).

**3. Reinforcement Layer :** The primary characteristic of the reinforcement layer is interface friction between it and the granular fill in which it is placed. As the granular layer deforms in shear, interfacial shear resistance,  $\tau$ , is mobilized which is expressed as

$$\tau = \mu \cdot \sigma \quad (39)$$

where,  $\mu =$  coefficient of friction, and  
 $\sigma =$  normal stress on the reinforcement layer

Implicit in this modelling process is the assumption that the relative displacement between the reinforcement and the granular fill is sufficient to mobilize (Fig. 24d) the full shear resistance (Madhav and Porooshab, 1988; Bourdeau, 1989). It is common knowledge in estimating shaft resistance of piles that the side or shaft resistance is fully mobilized at very small pile displacements. The frictional forces in the reinforcement layer generate tensile force,  $T$ , which is obtained by integrating or summing the mobilized interfacial shear stresses on both sides of the reinforcement, as

$$T = 2 \int \tau dA = 2 \sum \tau_i \Delta A_i \quad (40)$$

where,  $dA$  is the elemental area. Thus the reinforcement is modelled as a rough membrane.

Combining the soft clay (non-linear Winkler), granular fill (non-linear shear layer) and the reinforcement (membrane action through interfacial shear resistance) response (Fig. 24c), the governing equations for the RFB are obtained (Madhav and Poorooshasb, 1988 & 1989; Ghosh and Madhav, 1994a, b & c) for the plane strain case, as

$$q = \frac{(1 - \mu_b \tan \theta)}{(1 + \mu_b \tan \theta)} \cdot \frac{k_s w}{(1 + b_s w)} - \left[ \frac{(G_t H_t + G_b H_b)}{\{1 + b_s (dw/dx)\}^2} + \frac{T \cos \theta}{(1 + \mu_t \tan \theta)} \right] \frac{d^2 w}{dx^2} \quad (41)$$

$$\frac{dT}{dx} = -(\mu_t \cos \theta - \sin \theta) \left[ q + \frac{G_t H_t}{\{1 + b_s (dw/dx)\}^2} \right] \frac{d^2 w}{dx^2} - (\mu_b \cos \theta + \sin \theta) \frac{k_s w}{(1 + b_s w)} - \left[ \frac{G_b H_b}{\{1 + b_s (dw/dx)\}^2} \right] \frac{d^2 w}{dx^2} \quad (42)$$

where,  $G_t$  and  $G_b$  = shear moduli of the top and bottom layers or interfaces

$H_t$  and  $H_b$  = thickness moduli of the top and bottom layers or interfaces, and

$\mu_t$  and  $\mu_b$  = coefficient of shear resistance moduli of the top and bottom layers or interfaces.

Similar equations have been derived for the axi-symmetric case.

The boundary conditions are easily specified as the slope of the displacement curve is zero at the centre ( $dw/dx$  or  $dw/dr = 0$  at  $x$  or  $r = 0$ ) of the loaded region (symmetry) and the tensile force is zero ( $T = 0$  at  $x$  or  $r = L_r$ ) at the tip of the reinforcement (unstretched reinforcement). If it is possible to prestress the reinforcement, tensile force at the edge equals the prestress applied. Eqns 41 and 42 are solved by discretising the region of influence in to a number of elements and using the finite difference technique.

### *Confinement Effect*

With the application of load/stress or displacement to the RFB, it is

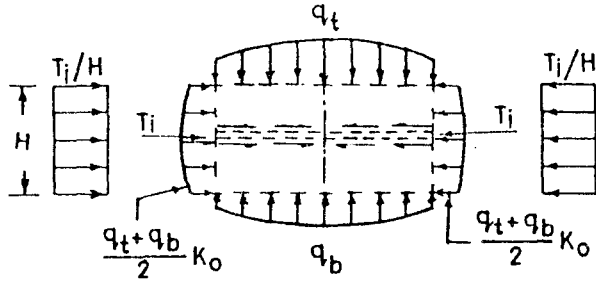


FIGURE 25 : Confinement Effect on Fill

very easy to represent the mobilization of interfacial shear stresses along the tensile forces in the reinforcement. The effect of the reinforcement on the response of the granular fill can be accounted for through what is termed as confinement effect. The confinement effect can be visualized from Fig. 25 where multiple layers of reinforcement are depicted for clarity of presentation. The tensile force in each layer of reinforcement increases from zero at its free end to a maximum value at the centre. Considering a small or finite length of the soil contained between two layers of reinforcement, apart from the normal stresses,  $q_t$  and  $q_b$ , each element is confined by lateral or horizontal stresses,  $T_i/H$  and  $K_o(q_t + q_b)/2$  (assuming  $K_o$  condition, i.e. no lateral displacement). A number of correlations are available (e.g. Hardin and Drnevich, 1972; Saxena and Reddy, 1989) for estimating the shear modulus of granular soil, as

$$G = C(\sigma_{av})^n \quad (43)$$

where,

$C$  = constant of proportionality,

$\sigma_{av}$  = average principal stress, and

$n$  = an exponent equal to 0.5 for small and 1.0 for large strains.

The governing equation for a Pasternak model with variable shear modulus (Madhav and Poorooshasb, 1989) is

$$q = \frac{k_s w}{(1 + \gamma w)} - \left[ \frac{HG(x)}{\{1 + b_s(dw/dx)\}^2} \right] \frac{d^2 w}{dx^2} - \left[ \frac{1}{\{1 + b_s(dw/dx)\}} \right] \left[ \frac{HdG(x)}{dx} \right] \left[ \frac{dw}{dx} \right] \quad (44)$$

*Generalized Model*

Based on the above derived equations, a generalized model for multi-layer reinforced granular fill-soft soil system is obtained (Ghosh, 1991). The generalized model incorporates the shear layer, membrane and confinement effects in a coupled manner (combined effect). The equations are solved easily by the finite difference technique.

*Results*

The predicted load-settlement response of a rigid circular footing on a reinforced granular fill is shown in Fig. 26. The unreinforced soft soil undergoes a normalized displacement of 0.125 at a normalized stress of 0.05. Due to the shear layer effect alone, the stress at the same displacement is about 0.1, nearly 100% improvement. The membrane action improves the response further to 0.11, a ten percent increase. The confinement effect

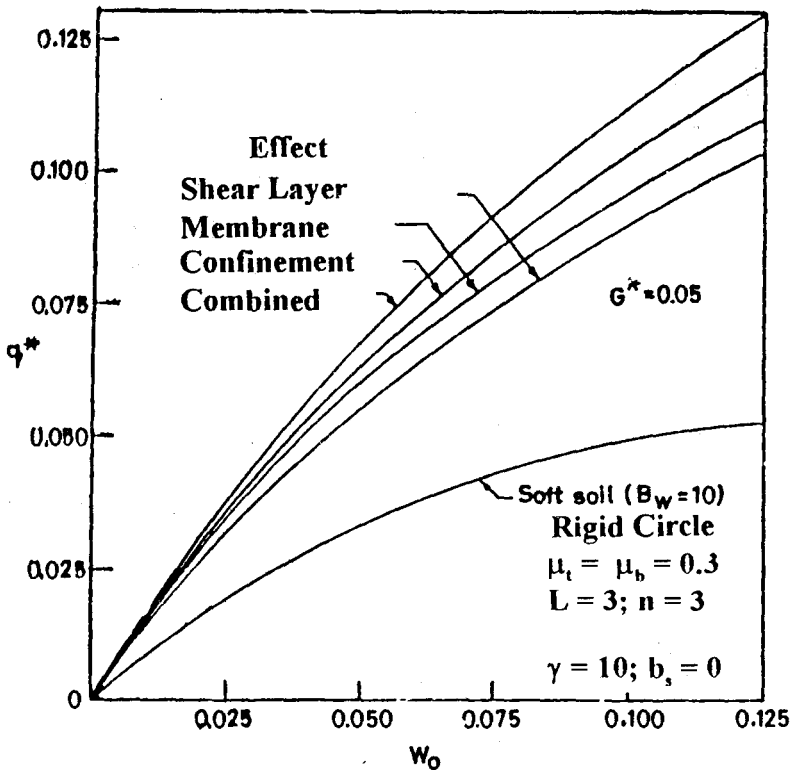


FIGURE 26 : Load-Settlement Response  
- Effect of Different Mechanisms

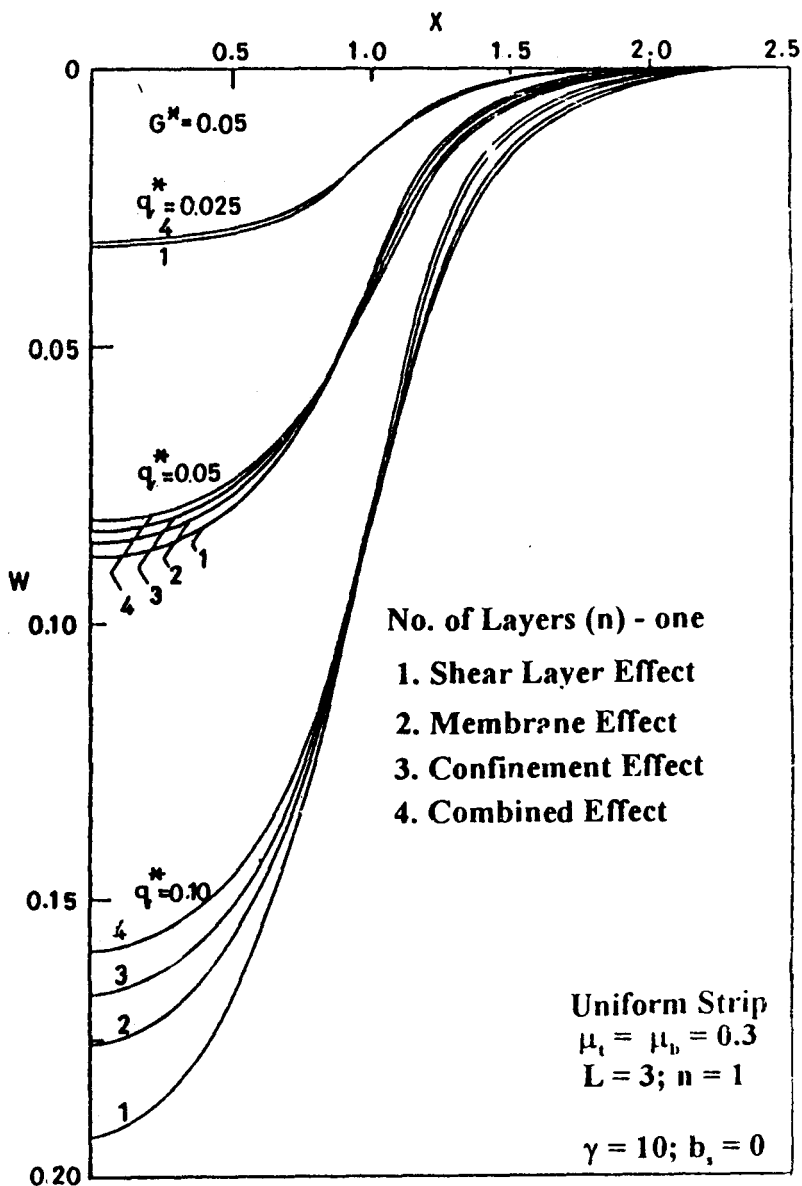


FIGURE 27 : Distance-Settlement Profiles

extends this stress to 0.116. The generalized model which couples all these effects and also their interactions, leads to a stress level of 0.13 for a displacement of 0.125. All the curves show a diverging trend indicating that these effects increase with either the stress level or at large displacements.

The distance-settlement profiles of a uniformly loaded strip are presented in Fig. 27 for a RFB with a single layer of reinforcement. At a low stress level ( $q^* = 0.025$ ), all the curves are close to each other and the contribution of the different effects is very small. The individual effects are discernible at moderate stress level of 0.05. The shear layer, the membrane, the confinement and the coupled effects cause a reduction of the central settlements and an increase in the settlements outside the loaded region. The RFB is tending towards increased rigidity with the mobilization of the above effects. At a relatively large stress level of 0.1, these effects are shown markedly. While the displacement with the shear layer effects alone is 0.19, the membrane, the confinement and the coupled effects reduce the central settlement to 0.176, 0.167 and 0.16 respectively.

The combined responses of all the mechanisms considered on a three layered RFB is compared (Fig. 28) for circular and strip loadings. The Soft soil is once again characterized by  $\gamma = 10$ . With a thin or less stiff granular layer ( $G^* = 0.05$ ), the stress on a uniformly loaded strip corresponding to a displacement of 0.125 is 0.074. The stress level increase to 0.085 for three layers of reinforcement. The corresponding stresses for a circular footing increase from 0.104 to 0.13. For thicker or stiffer granular fills ( $G^* = 0.2$ ), the confinement mechanism predominates and the coupled mechanisms lead to a significant improvement in the stress-settlement response of the footings (both strip and circular ones). Compared to the effects in the plane strain case (strip footing), the contributions of the coupled mechanisms are significantly more in the case of circular footing (axi-symmetric case) because of the substantial increase in the confinement of the granular fill due to stress transfer at the granular fill-soil interface. This modelling approach of representing RFB on soft soil has been extended for compressible granular fills by Shukla and Chandra (1994 and 1995) and for extensible reinforcement by Yin (1997).

#### **Modelling IV : Micromechanisms – Reinforcement Strip – Soil Interactions**

In the present section, following Madhav and Pitchumani (1992, 1994 and 1996) and Pitchumani (1992) reinforcement strip-soil interaction mechanisms are postulated and using a continuum approach analyzed for interfacial stresses. Subsequently, the reductions in settlements of reinforced soil beds are estimated. The mechanisms that operate in reinforced foundation beds have been identified as follows. The applied surface load or stress,

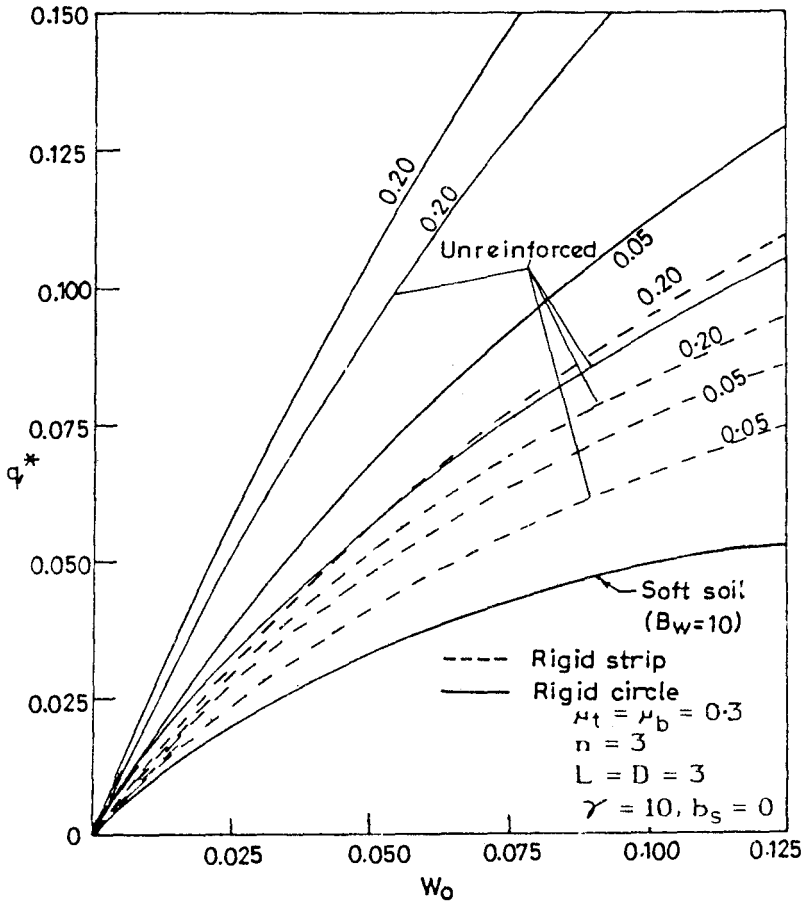


**FIGURE 28 : Comparison of Load-Settlement Responses of Rigid Strip and Circular Plates on RFB**

induces downward and lateral movement of the soil. The reinforcement placed at some depth, experiences vertical deformation and lateral extension. Depending on its axial and normal stiffness, the reinforcement resists the soil displacements and consequently mobilized both shear and normal stresses at the interfaces. These interaction stresses in turn prevent or reduce deformations of soil leading to reductions in surface settlements and lateral deformations of the soil.

#### *Single Strip : Shear Interaction*

A rectangular area,  $2L_f \times 2B_f$ , transmits a uniform stress of intensity,  $q$ , on the surface of a semi-infinite continuum (Fig. 29) whose modulus of deformation is  $E_s$ , and the Poisson's ratio,  $\nu_s$ . An inextensible reinforcement

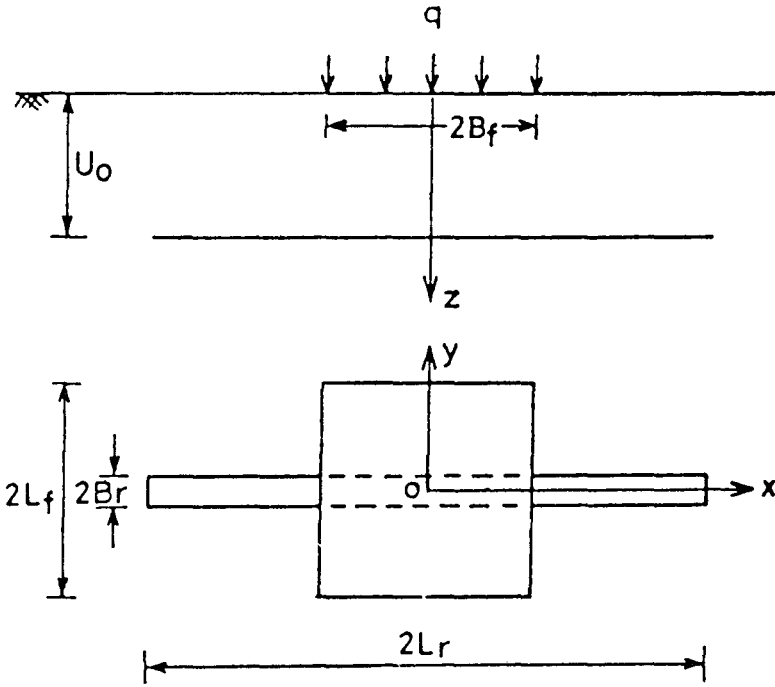


**FIGURE 29 : Definition Sketch – Single Strip**

strip,  $2L_f \times 2B_r$ , is placed centrally below the loaded area at a depth  $U_0$ . The width of the strip,  $B_r$ , is small relative to its length and the thickness,  $t_r$ , negligible. The shear stresses mobilized at the reinforcement strip-soil interface are assumed to be constant over the width and to vary only along its length. In the first instance, the displacements of the strip in the vertical direction (i.e. with respect to the normal stresses acting on the strip) are assumed to have no effect on the shear interactions. Under the action of the applied stresses, the soil below the surface has a tendency to move laterally outward. The interactions stresses on the soil and on the reinforcement strip are depicted in Figs. 30a and 30b respectively. The stresses are directed inward for the soil as they oppose the outward movement and are directed outward of the strip. Due to symmetry, only half the length of the strip need be considered. The strip is divided into  $N$  elements, each of size  $dl = L_f/N$ . The shear stress on the element 'j' is  $\tau_j$ .

**Analysis**

The net horizontal displacement of node  $i$ , is the algebraic sum of the displacements due to the applied surface stress,  $q$  and the interaction stresses,

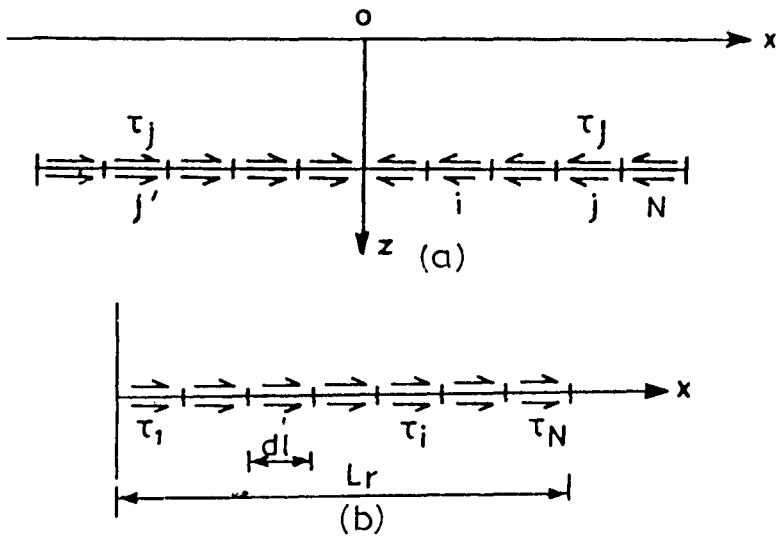


FIGURE 30 : Interaction Stresses on (a) Soil; and (b) Reinforcement Strip

$\tau_j$ . The former are computed by integrating Boussinesq solution for a point force on the surface and the latter from the Mindlin's solution for a horizontal load below the surface of a semi-infinite medium. While calculating the latter, the effects of the stresses on either (left and right of the centre) side of the reinforcement strip are considered. The integrations are carried out numerically over the area of the strip.

### *Inextensible Strip*

If the modulus of elasticity,  $E_r$ , of the reinforcement strip is very large in comparison to that of the soil, the strip is treated to be inextensible. For

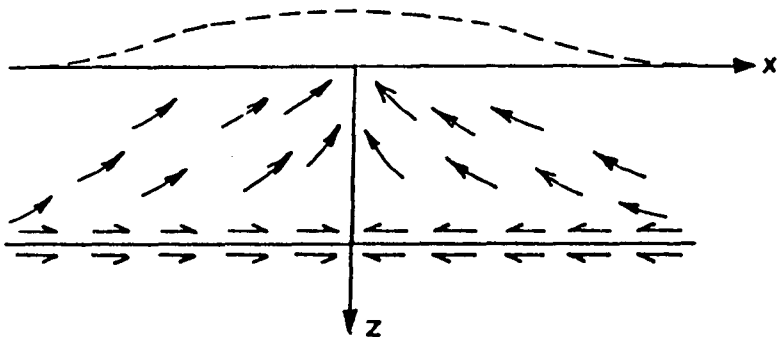
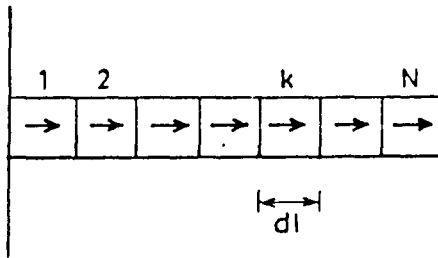


FIGURE 31 : Reduction of Settlement at Surface

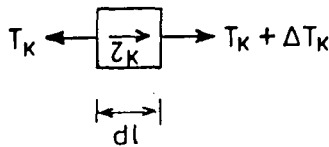
an inextensible strip, the net horizontal displacements are zero. The compatibility of displacements requires that the displacements of the points in the soil along the interface are also zero. A set of simultaneous equations obtained, and solved for the interaction shear stresses. Once the interaction stresses along the strip are evaluated, they are integrated using Mindlin's solution to compute the vertical surface displacements (Fig. 31) which are directed upward and are equivalent to a reduction in surface settlements

**Extensible Strip**

The reinforcement strip has a finite modulus of elasticity,  $E_r$ . The ratio  $E_r/E_s$ , if moderate, the extension of the strip needs to be incorporated in the analysis. The net lateral displacements of the points in the soil along the strip are calculated as before. Since the strip is extensible, the tensile force in it at the centre of each element is calculated by summing up the shear stresses (Fig. 32). The elongations in the strip at each of these nodes are obtained from the tensile forces acting along its length. The compatibility of deformations require that the displacements of the strip and the soil along the nodes on the interface should be the same (no slip condition). Therefore, equating the expressions for the soil and strip displacements at the nodes, a



(a)



(b)

**FIGURE 32 : Integration of (a) Shear Stresses on and (b) for Tension in the Reinforcement**

set of equations are obtained which are solved once again for the interaction shear stresses and from them the surface upward displacements. In this case, the shear stresses and the surface displacements are functions of a relative extensibility parameter,  $K_r = E_r t_r / E_s B_f$ , which accounts for the axial stiffness of the strip, the modulus of deformation of the soil and the width of the applied stress on top.

### *Single Strip : Normal Stress Interaction*

The stress applied on the surface causes the soil underneath to deform as shown in Fig. 33. The settlements near the centre would be large and decrease with distance from there. If the reinforcement strip is very flexible, its deformed shape conforms to that of the settlement profile of the soil. However, if it is rigid, the strip would undergo a rigid body displacement,  $\delta_0$ , as shown in Fig. 33, much like the settlement of a rigid footing on soil. To achieve a uniform displacement, normal stresses are mobilized on the strip once again very much like the contact stresses between a footing and the soil. The strip transfers the load from the centre to the edges to realize uniform settlement profile. The mobilized interfacial normal stresses represent the difference between the normal stresses on the top and the bottom faces of the strip. The net result of these normal stresses is to push the soil above upward near the centre of the loaded area resulting in a reduction in the surface settlements.

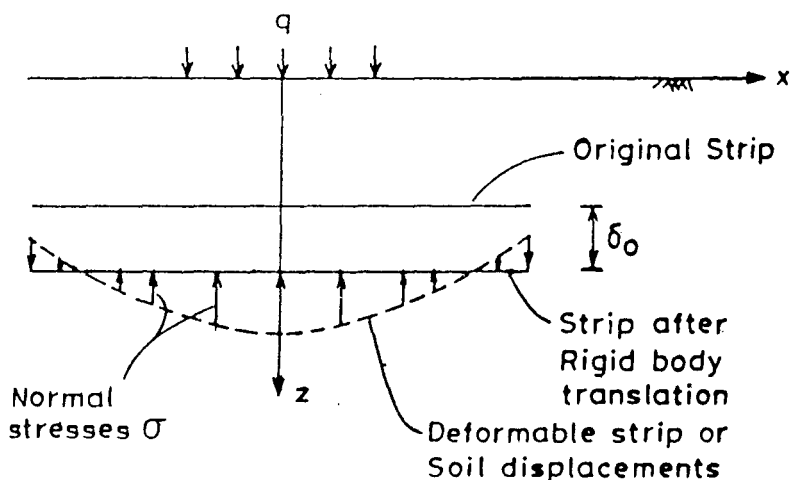


**FIGURE 33 : Rigid Strip beneath a Loaded Area**

**Analysis**

The method of analysis for this case is very similar to the previous case (shear interaction). Instead of considering lateral or horizontal displacements, vertical displacements are evaluated from Boussinesq solution and the Mindlin's solution for a vertical point load within an elastic continuum. The vertical displacement of point along the strip due to applied surface stress are computed from the Boussinesq solution. The displacements due to the interaction normal stress,  $\sigma_j$ , (Fig. 33) are evaluated by integrating Mindlin's solution. Another difference between shear and normal stress interaction solutions is that in the former, the mobilized interaction shear stresses on either side of the centre cause movements in opposite direction, while the interaction normal stresses on either side of the strip cause the deformations of the same sign. The compatibility of deformations requires that all the nodes along the strip settle by a uniform value of  $\delta_0$ . A set of N simultaneous equations are obtained for N unknown interaction normal stresses. However, in this case, there is one more unknown, the rigid body displacement or settlement of the strip,  $\delta_0$ . To solve for this, the equilibrium equation is invoked. Since no external force acts on the strip, the sum of the normal stresses acting on the strip is zero. These N + 1 set of equations are solved for the interaction normal stresses and the rigid body displacement. From the newly found normal stresses, the surface displacements (reductions in settlements) are once again evaluated by integrating Mindlin's solution.

**Flexible Reinforcement Strip**

If the reinforcement strip is not rigid but is flexible, it acts like a beam and deforms as shown in Fig. 34. The flexural rigidity or stiffness of the strip is represented by  $E_r I_r$ , where  $I_r$  is the moment of inertia of the strip cross sectional area. The net soil displacements along the nodes of the strip are calculated as before. The strip displacements are calculated using the beam equation

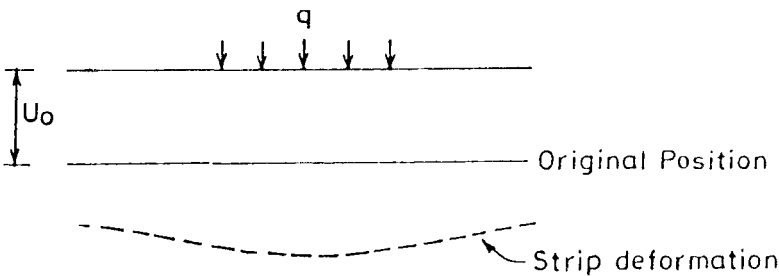


FIGURE 34 : Deformation of Flexible Strip Area

$$E_r I_r \frac{d^2 w}{dx^2} = M_b \quad (45)$$

where,  $w$  = strip displacement in the vertical direction at a distance  $x$  from the centre, and

$M_b$  = bending moment due to the normal stresses.

The boundary conditions for the beam are (i) at the centre, i.e.  $x = 0$ , the slope is zero from symmetry, and (ii) at the edge of the strip, i.e.  $x = L_r$ , the bending moment is zero ( $d^2 w/dx^2 = 0$ ). The beam equation (Eqn. 45) in finite difference form is

$$E_r I_r \left[ \frac{w_{i-1} - 2w_i + w_{i+1}}{\Delta t^2} \right] = M_{bi} \quad (46)$$

where,  $w_{i-1}$  = displacements to the left of any node  $i$ ,  
 $w_i$  = displacements at any node  $i$ ,  
 $w_{i+1}$  = displacements to the right of any node  $i$ , and  
 $M_{bi}$  = bending moment at node  $i$ .

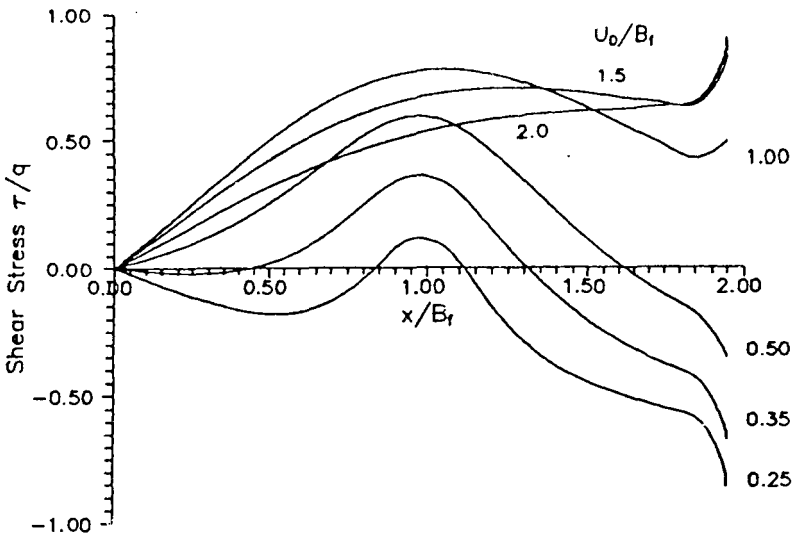


**FIGURE 35 : Variation of Shear Stresses with Distance**  
 - Effect of  $U_0/B_f$  ( $L_r/B_f = 2$ ,  $L_f/B_f = 1$  and  $\nu_s = 0.3$ )

The beam equation is written in terms of the  $N + 1$  nodal displacements of the strip and the compatibility of displacements are satisfied by equating the soil and the strip displacements. The mobilized normal interaction stresses are evaluated by solving the  $N + 1$  simultaneous equations. The equilibrium of vertical forces is incorporated within the beam equation.

### *Interaction Shear Stresses*

The variation of normalized shear stress,  $\tau/q$ , with normalized distance,  $x/B_f$ , along the strip for various depths of placement,  $U_0/B_f$ , are depicted in Fig. 35, for a strip of length,  $L_f/B_f = 2$ , placed below a square loaded area,  $L_f/B_f$ . The mobilized shear stress acts on the top and the bottom faces of the strip in equal proportion. The shear stress is positive if it prevents outward lateral movement and as such is directed inwards. The shear stress at the centre is zero as it should be. For strips at shallow depths,  $U_0/B_f = 0.25$ , the shear stresses are negative over a large portion of the strip and thus do not contribute to improvement. Positive shear stresses are mobilized only for  $x/B_f$  in the range of 0.85 to 1.1. With increasing depths of placements, the shear stresses are positive over most of the length of the strip. The sharp increase in shear stresses at the extreme edge of the strip ( $L_f/B_f = 2$ ) is because the strip is assumed to be inextensible. This result is in consonance with the infinite contact stresses predicted at the edges of rigid footings. The shear stresses increases with distance and peak at points below the edge of the loaded area. They are a maximum for depth of placement of  $U_0 = B_f$ . The effectiveness of the reinforcement reduces for depths in excess of  $B_f$ . These results are verified by many experimental studies reported in literature.

The effect of the length of the strip,  $L_f/B_f$ , on the mobilization of shear stresses, is investigated in Fig. 36 for a strip at  $U_0/B_f = 1.0$ . for short strip ( $L_f/B_f = 1$ ) the stresses increase almost linearly over the length of the strip. for longer strips, the shear stress increases to a value of about  $0.8q$  at  $x/B_f = 1.0$  (beneath the edge of the loaded area) and decrease monotonously beyond. For strips of length,  $L_f/B_f = 2.0$ , the shear stresses are positive throughout. No extra advantage accrues by extending the length of the strip beyond 3.0 to 4.0 times the width of the loaded area, an experimentally verified fact.

### *Tension in the Reinforcement*

The mobilized shear stresses, in turn, produce tension in the reinforcement strip. The tensile force,  $T_i$ , at the centre of the element  $i$ , is the sum of the forces due to shear stresses on either side of the strip and is obtained from Eqn. 40. The tension is a maximum at the centre and zero at the edge of the strip. The variation of normalized tension in the strip,  $T/qB_f^2$ ,

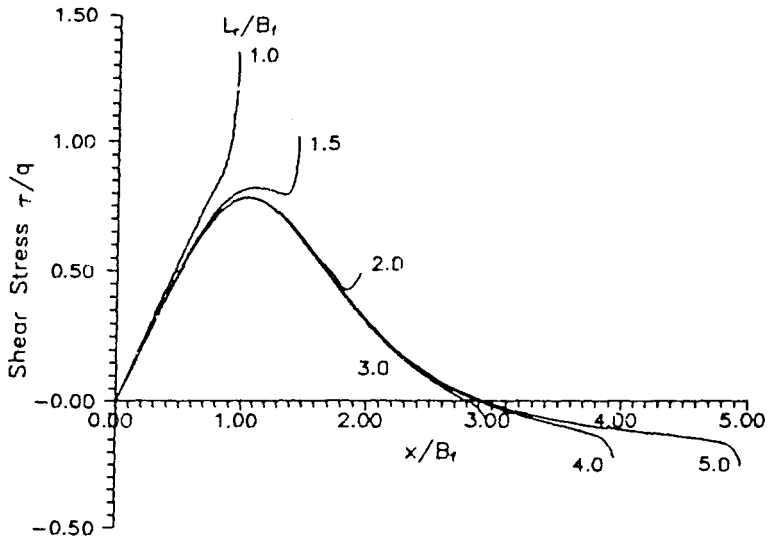


FIGURE 36 : Variation of Shear Stresses with Distance  
 - Effect of  $L_f/B_f$  ( $U_0/B_f = 1$ ,  $L_f/B_f = 1$  and  $\nu_s = 0.3$ )

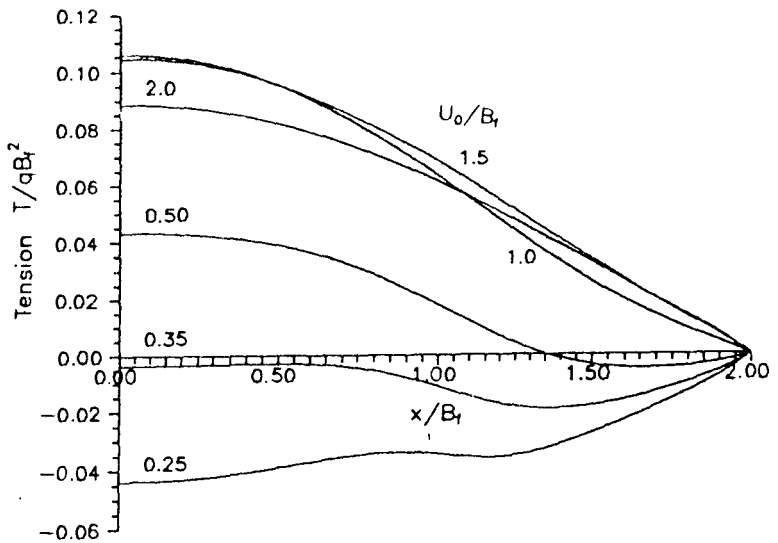


FIGURE 37 : Variation of Tension with Distance  
 - Effect of  $U_0/B_f$  ( $L_f/B_f = 2$ ,  $L_f/B_f = 1$  and  $\nu_s = 0.3$ )

along the strip length, can be seen in Fig. 37. For strips placed at depths,  $U_0 < 0.35B_f$ , compressive forces instead of tension, are developed in the strip as the soil displacements are inward and not outward. Strips placed at shallow depths are ineffective in reinforcing soil based on shear interaction alone. Maximum tensile force of  $0.105qB_f^2$ , is mobilized at the centre for a strip placed at  $U_0 = B_f$  as a result of mobilization of maximum shear stresses. Strips placed at depths beyond  $0.5B_f$  are subjected to tension over their full lengths.

### *Settlement Reduction*

For the mobilized shear stresses,  $\tau_j$ , the displacements of the points on the surface are computed by integrating Mindlin's solution for a horizontal load beneath the surface in a semi-infinite medium. The displacement,  $\rho_{zk}$ , at any point k, on the surface is

$$\rho_{zk} = q B_f \cdot (SRC_k / G_s) \quad (47)$$

where,  $SRC_k$  = settlement reduction coefficient at node k, and

$G_s$  = shear modulus of the soil.

SRC at the centre of the loaded area, O, is defined as  $I_{sc}$ . Figure 38 depicts the variation of ERC along the x direction on the surface, for strips of various lengths and for a depth of placement of  $U_0/B_f = 1.0$ . The settlement reduction is maximum at the centre of the loaded area, O, for all lengths of reinforcement and reduces with distance from the centre. SRC increases with increasing lengths of the strips. The improvement in SRC for  $L_f/B_f$  increasing from 1 to 2 is 0.0023 to 0.00315 and significant. With further increase in the length of the strip from 2 to 5 times  $B_f$ , SRC increases to only 0.00348. This insignificant increase in SRC confirms experimentally established fact that only marginal improvement occurs by increasing the strip length beyond twice the footing width.

**Extensible Strip :** For extensible strips, the results (Fig. 39) are dependent on the relative extensibility parameter,  $K_r (= E_r t_r / E_s B_f)$ .  $K_r = 0$  indicates no reinforcement (unreinforced soil) in which case no shear stresses are mobilized.  $K_r$  equal to infinity implies a rigid strip and the results agree with those from Fig. 35. For all values of the ratio,  $K_r$ , the mobilized shear stresses are maximum beneath the edge of the loaded area. They decrease with decreasing values of  $K_r$  showing lesser effect of the reinforcement. The sharp increase in the mobilized shear stress is observed for all values of  $K_r$ .

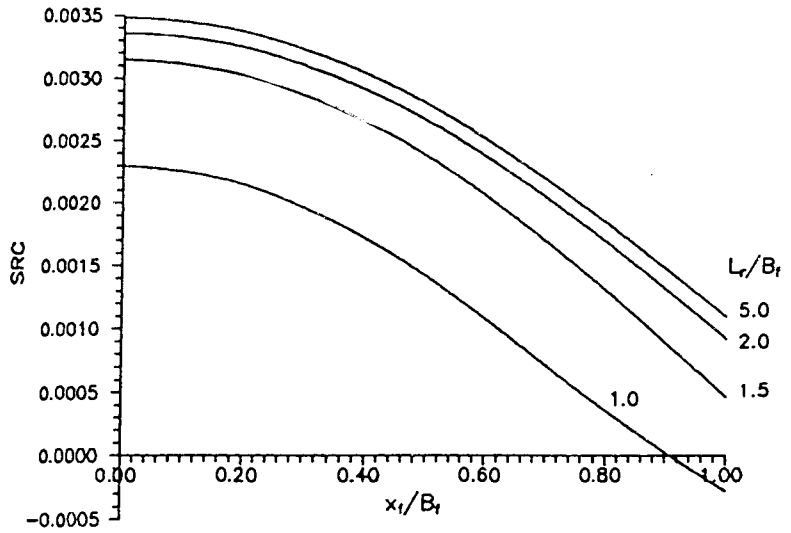


FIGURE 38 : Variation of SRC with Distance  
 - Effect of  $L_f/B_f$  ( $U_0/B_f = 1$ ,  $L_f/B_f = 1$  and  $\nu_s = 0.3$ )

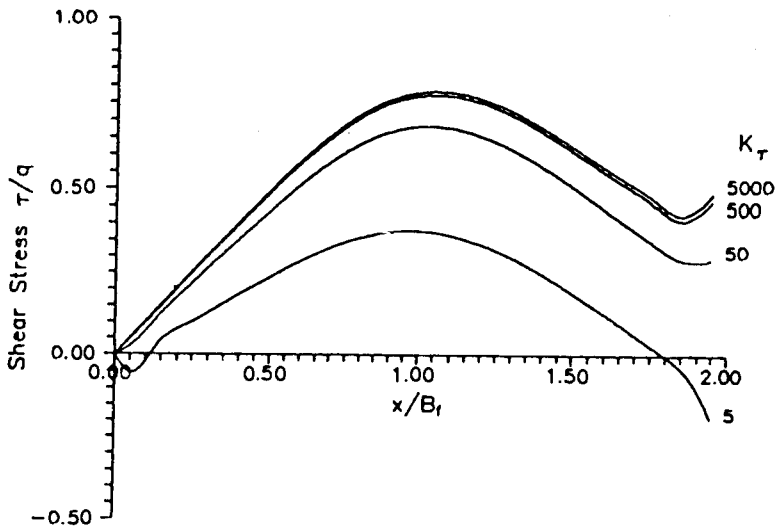


FIGURE 39 : Effect of Extensibility on Shear Stresses

### *Interaction Normal Stresses*

The variation of the normalized stress,  $\sigma/q$ , with distance,  $x/B_f$ , along the half length of a strip for different depths of placement,  $U_0/B_f$ , below a square loaded area and for strip of length of  $L_f/B_f$  of 2, is presented in Fig. 40. A positive stress acts upward and prevents or reduces settlements. Maximum normal stresses are mobilized at the centre where the settlement of unreinforced soil would have been the largest. The normal stresses decrease with distance from the centre, change sign close to the edge of the loaded area and become negative over the strip beyond the loaded area. If  $U_0/B_f$  is zero, the strip is at the surface and become a part of the footing. The effect of the strip considering normal stress interaction is maximum for strips located close to the surface. The effect reduces with the depth of placement unlike the case which considers shear interactions (the interaction shear stresses are maximum for a depth of placement of  $B_f$ ). For shallow depths of placement of the strip, the normal stresses are uniformly large, of the order of four to five times the applied load intensity, beneath the loaded area, decrease rapidly near its edge and once again are large and negative outside. The sharp increase of the normal stress close to the tip of the reinforcement is once again as it should be for rigid foundations.

For a given depth of placement ( $U_0 = B_f$ ) of the strip, the mobilized normal stresses are very sensitive the length,  $L_f/B_f$ , of the strip (Fig. 41). The variation of normal stress with distance,  $x$ , is same as discussed with respect to Fig. 40. The point beyond which the normal stresses become negative shifts away from the centre with increasing lengths of the strip. If the transition is close to the edge of the loaded area for  $L_f/B_f$  equal to 2, the point moves to  $1.8B_f$  for  $L_f/B_f$  of 5.0 implying that longer the strips the better is the improvement. However, the mobilized normal stress at the centre increase with increasing length of the strip since the displacements have to be maintained uniformly over longer lengths of the strip.

### *Settlement Reduction*

The effect of the length of the rigid strip,  $L_f/B_f$ , placed at a depth  $U_0/B_f = 1.0$ , below a square loaded area, on SRC, can be seen in Fig. 42. The SRC values are a maximum at the centre of the loaded area and decreases gradually with distance from the centre from all lengths of the strips. The settlement reduction is least at the edge of the loaded area. SRC values increase with increase in the length of the strip. SRC at the centre are 0.007, 0.0082 and 0.013 for  $L_f/B_f$  values of 1, 3 and 5 respectively. The increase in SRC with  $L_f/B_f$  follows from the mobilized normal stresses which also are higher for longer strips.

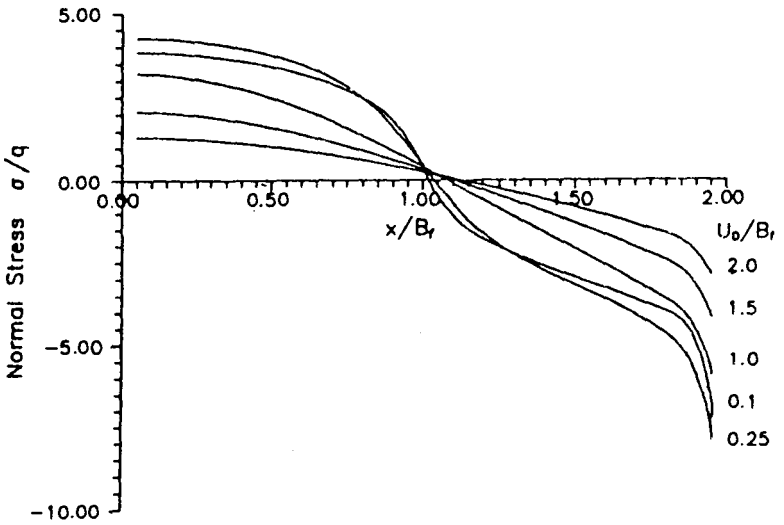


FIGURE 40 : Variation of Normal Stress with Distance  
 - Effect of  $U_0/B_f$  ( $L_r/B_f = 2$ ,  $L_f/B_f = 1$  and  $\nu_s = 0.3$ )

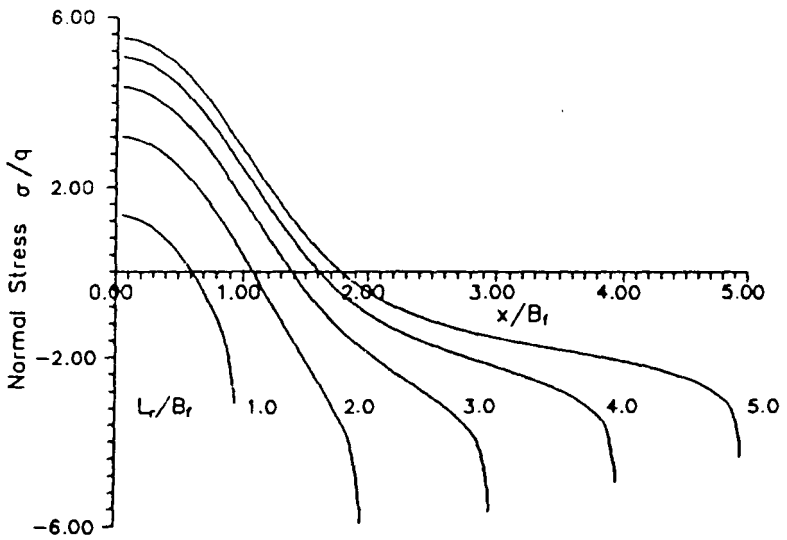


FIGURE 41 : Variation of Normal Stress with Distance  
 - Effect of  $L_r/B_f$  ( $U_0/B_f = 2$ ,  $L_f/B_f = 1$  and  $\nu_s = 0.3$ )

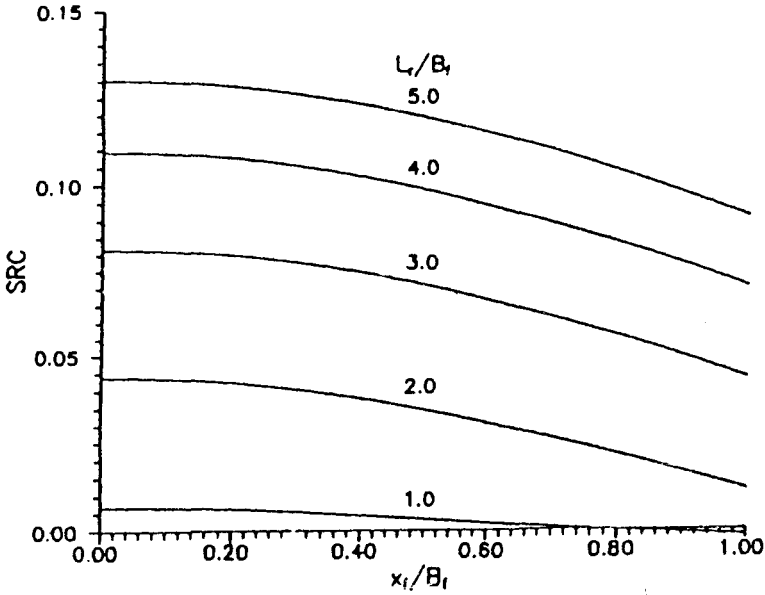


FIGURE 42 : Effect of  $L_r/B_f$  on SRC vs. Distance Relation ( $U_0/B_f = 1$ ,  $L_r/B_f = 1$  and  $\nu_s = 0.3$ )

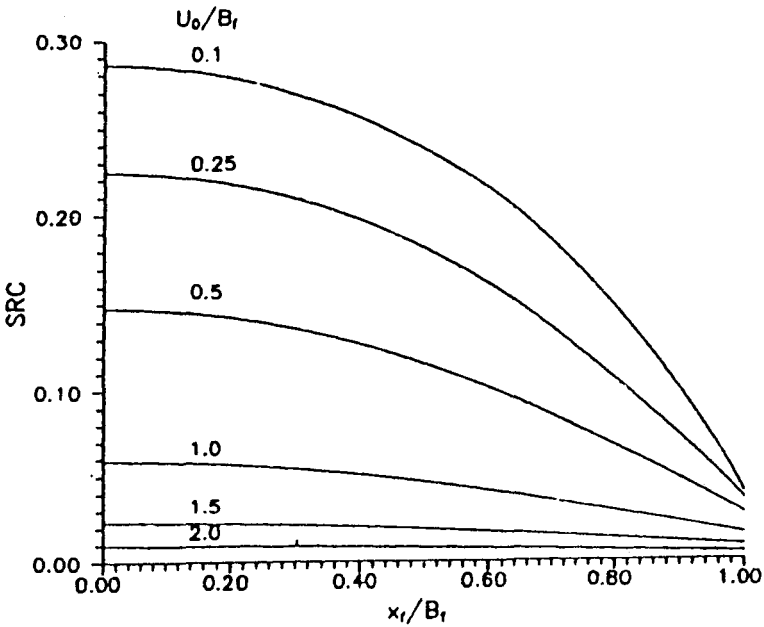


FIGURE 43 : Effect of  $U_0/B_f$  on SRC vs. Distance Relation ( $L_r/B_f = 2$ ,  $L_r/B_f = 1$  and  $\nu_s = 0.3$ )

Figure 43 presents the effect of depth of placement of the reinforcement strip of length,  $L_f/B_f = 2$  on SRC. Unlike in shear interactions where the SRC is a maximum at some optimal depth of  $U_0/B_f = 1.0$ , SRC in case of normal stress interaction is maximum for a strip at the surface and decreases with the depth of placement. SRC is maximum at the centre of the loaded area and decreases to near zero values at the edge of the loaded area. For depths of placement of the strip in excess of  $1.5B_f$ , SRC values are small and uniform over the half width of the applied loaded area. For purpose of design, the central settlement reduction coefficient,  $I_{sc}$  is plotted with  $U_0/B_f$  for different aspect ratios of loaded area and for a strip of length  $L_f = 2B_f$  in Fig. 44.  $I_{sc}$  values decrease with  $U_0/B_f$  for all  $L_f/B_f$  ratios. They increase with the ratio,  $L_f/B_f$ , of the loaded area. However, the reductions for  $L_f/B_f$  greater than 2.0 are not significantly different from those for  $L_f/B_f = 2$  for the given length of the strip.

### *Displacement of Strip*

It is interesting to determine the position of the strip due to the applied surface load. The displacement,  $\delta_0$ , of the reinforcement strip is normalized with  $q \cdot B_f/E_s$ . The normalized displacement,  $\delta_0 \cdot E_s/q \cdot B_f$ , decreases (Fig. 45) with depth of placement,  $U_0/B_f$ , and with increase in length of the strip  $L_f/B_f$ . For a strip of length  $L_f = B_f$ , the normalized displacements are 1.78 and 0.85 for depths of placements,  $U_0/B_f$  of 0.1 and 2 respectively. The corresponding values for a longer strip ( $L_f/B_f = 5$ ) are 0.72 and 0.5 respectively.

### *Flexible Strip*

The strip, as mentioned earlier, can be modelled to behave like a beam. Equation 45 is solved in finite difference form (Eqn. 46) to arrive at the mobilized normal stresses, SRC and the displacements of the strip. A new parameter,  $K_B$ , defined as  $K'_B = E_r I_r / E_s \cdot B_f^4$ , represents the relative strip flexibility.  $K_B$  values of zero and infinity imply no and rigid reinforcement strips respectively. Figure 46 represents the variation of the normalized normal stress,  $\sigma/q$ , with distance,  $x/B_f$ , for different values of the relative flexibility ratio,  $K_B$ , for strips of length,  $L_f/B_f$ , of 2, placed below a square area at a depth  $U_0 = B_f$ . The mobilized stresses for strips with low values of  $K_B$  ( $< 10^{-2}$ ) are nearly zero which means negligible effect of the strip as it is very flexible. The normal stresses increase with increasing values of  $K_B$  and tend to close to those for a rigid strip for  $K_B > 2$ . Therefore, for practical purposes,  $K_B = 2$  can be considered to represent a rigid strip. The pattern of variation of normal stresses with distance is the same as observed for rigid strips (Fig. 40). A maximum positive value is mobilized at the centre of the strip, the normal stress becomes close to zero beneath the edge and tends to very large negative values at its edge (edge effect). For low values of  $K_B$ , the

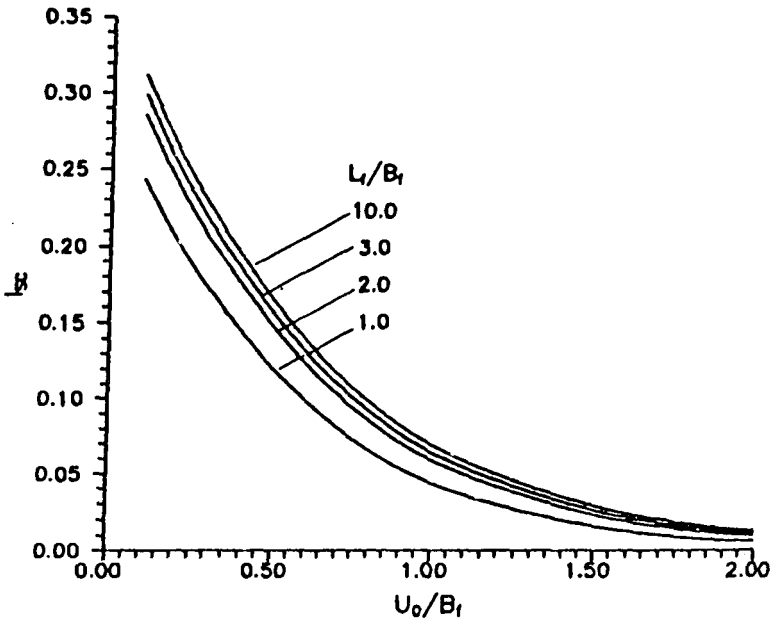


FIGURE 44 : Effect of Aspect Ratio  $L_r/B_f$  on  $I_{sc}$   
 ( $L_r/B_f = 2$  and  $\nu_s = 0.3$ )

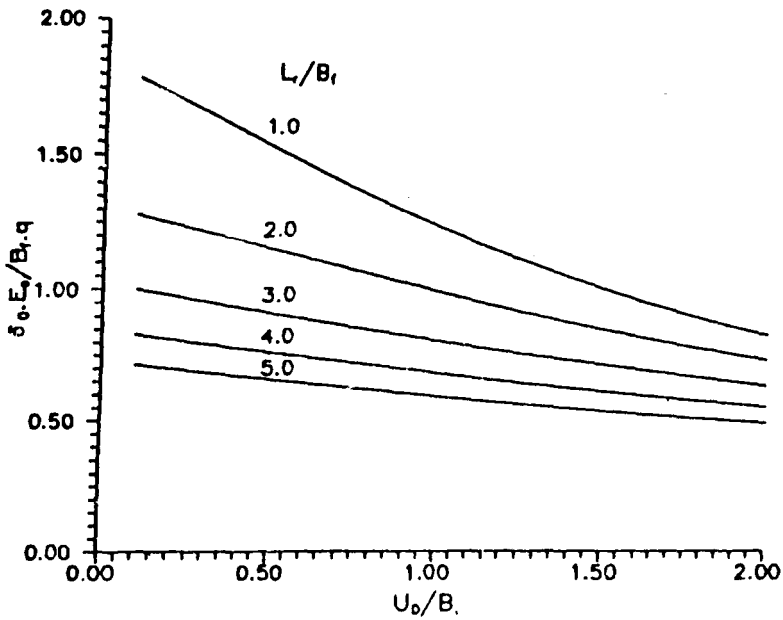


FIGURE 45 : Effect of Depth of Placement on Strip Displacement  
 ( $L_r/B_f = 1$  and  $\nu_s = 0.3$ )

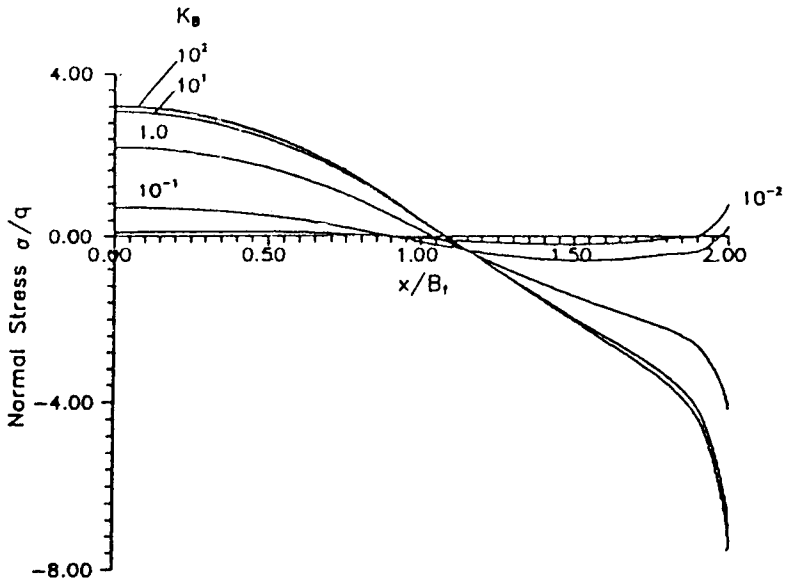


FIGURE 46 : Variation of Normal Stress with Distance  
- Effect of  $K_B$  ( $U_0/B_f = 1$ ,  $L_r/B_f = 2$  and  $L_f/B_f = 1$ )

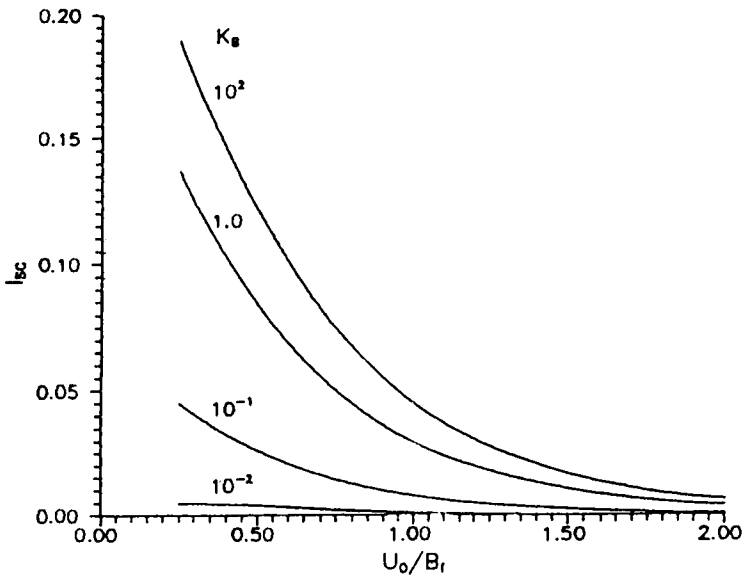


FIGURE 47 : Effect of  $K_B$  on  $I_{sc}$  ( $L_r/B_f = 2$ ,  $L_f/B_f = 1$  and  $\nu_s = 0.3$ )

difference between the soil and strip deflections being small, the normal stresses mobilized to counteract this difference in displacements, are small. As  $K_B$ , increases, the difference between the soil displacements due to applied surface loading alone and the actual strip deflections are high, and hence, the stresses mobilized also are large.

The effect of  $K_B$  on settlement reduction at the centre of the loaded area,  $I_{sc}$ , for different depths of placements  $U_0/B_f$ , for a strip of length of  $L_r = 2B_f$ , can be seen in Fig. 46. The trends of the curves are very similar to those for a rigid strip (Fig. 42). In fact, the curve for  $K_B = 2$  agrees closely with that for a rigid strip. The influence of the strip in reducing settlement at the centre decreases with decreasing values of the flexibility ratio,  $K_B$ .

## Conclusions

The paper introduces some ideas concerning the modelling process which is used often to represent a physical phenomenon or response. Geotechnical Engineers have been using models to study many of the complex problems. Modelling requires a proper visualization of the mechanisms and an understanding of the problem. It is a continuous process in that the model is upgraded to simulate as closely as possible the real situation. A model can be built or developed by first analyzing the physics of the problem and then identifying the mechanisms operating and/or characteristics of the system under study.

Amongst the various (physical, analytical/numerical, centrifuge, etc.) modelling techniques available, a simple modelling approach, the shear layer concept, has been utilized to analyze the effect of the non-homogeneity of a granular pile on its response. The granular pile is treated as a compressible pile and the soil as a series of shear layers. With this model, it has been possible to carry out numerical experimentation to quantify the effects of various parameters, e.g. the rate of increase in the modulus of deformation of the granular pile with depth, its length to diameter ratio, the response of the soil (linear/non-linear), etc. on the overall behaviour.

One major application of geosynthetic reinforcement in the form of geogrids, geonets by themselves or in combination with bamboo or rope fascines, is for the construction of embankments, working platforms and unpaved roads on soft soil. RFB increases the stability of embankments and working platforms and the bearing capacity in the case of unpaved roads. The different mechanisms postulated for the estimation of bearing capacity of geosynthetic reinforced granular fill - soft soil system are reviewed. They encompass the membrane action which is possible only at large rut depths, and the lateral thrust and shear layer approaches valid for small or negligible

rut depths. A recently proposed theory based on the shear resistance of granular layer, the confinement due to reinforcement force and the additional surcharge effect from the stresses transferred to the soil outside the loaded area, appears to predict the bearing capacity reasonably.

The gross or the global response of a foundation resting on a subgrade or on a reinforced foundation bed can be easily studied by the mechanical models which can be built up using the basic model elements, the Winkler springs, the Pasternak shear layer and the rough membrane proposed by Madhav and Poorooshasb. The shear stiffness of the granular layer, the membrane action of the reinforcement, the confinement effect arising from the interaction between the reinforcement and the granular fill, are accounted for in the modelling process. Reinforcement of soil not only strengthens by its inherent characteristic but also modifies the stress conditions in the soil and improves its performance, unlike in R.C.C., where only the reinforcement action alone is realized. Coupling of all these interactions in to a generalized model have been shown to contribute to the overall response of the RFB.

The micro-mechanisms operative between a reinforcement strip and the soil in which it is embedded are analyzed by the continuum modelling technique developed. Both the shear and normal stress interactions with inextensible and extensible and rigid and flexible reinforcement have been quantified in terms of stresses mobilized and reductions in settlements of the points on the surface where the loads are acting. Many of the experimental observations such as the effects of the depth of placement of reinforcement, the length of reinforcement relative to the width of the loaded area, the extensibility or flexibility of reinforcement, etc. are corroborated by the results of this numerical modelling approach.

### **Acknowledgement**

The academic environment and freedom fostered at the Indian Institute of Technology, Kanpur, by successive Directors and the Heads of the Departments of Civil Engineering, has greatly helped in carrying out the work reported in this paper. My colleagues, some of them former students have greatly contributed to the development of the ideas and techniques presented here. Interactions with Profs. Basudhar, Sarvesh Chandra, Kameswara Rao, Valsangkar and Yudhbir are gratefully acknowledged. Former post-graduate students Drs. C. Ghosh, N.K. Pitchumani, J.S. Sharma, N. Sabhahit, P.P. Vitkar, (Late) Kurma Rao and Sri K.U. Rao, to name a few have carried out some of the ideas to fruition. The author's stay at University of Sydney, Australia; Concordia, Canada; Ghent, Belgium; and Saga, Japan and interactions with Profs. H.G. Poulos, E.H. Davis, H.B. Poorooshasb, W.F. Van Impe and N. Miura and regular visits to I.I.Sc., Bangalore for interaction and trying out the results with the colleagues there had a significant influence

on this work. Sarojini, 'Dear' to me, along with daughters Rajani and Neeraja not only bore with fortitude the demands of time and separation demands in the pursuit of research, but gave support and encouragement necessary and needed for this effort. J.K. Sharma, L. Balamurali and K.P. Sujata helped with the editorial work. Sri J.C. Verma was always ready for the drafting of the figures.

## References

- ALAMGIR, M., MIURA, N., POOROOSHASB, H.B. and MADHAV, M.R. (1996) : "Deformational Analysis of Soft Ground Reinforced by Columnar Inclusions", *Computers and Geotechnics*, Vol.18, No.4, pp.267-290.
- BARAN, P.A. and SWEEZY, P.M. (1968) : "Monopoly Capital : An Essay on the American Economic and Social Order", Harmondsworth, Penguin Books (*from Soil Behaviour and Critical State Soil Mechanics* by D.M. Wood, Cambridge Univ. Press, 1990).
- BARDEN, L. (1965) : "Consolidation of Clay with Non-linear Programming", *Geotechnique*, Vol.15, p.345-362.
- BASUDHAR, P.K., VALSANGKAR, A.J. and MADHAV, M.R. (1979) : "Optimal Lower Bound of Passive Earth Pressure using Finite Elements and Non-linear Programming", *Int. Journal of Num. and Analytical Methods in Geomechanics*, Vol.3, pp.369-379.
- BOURDEAU, P.L. (1989) : "Modelling of Membrane Action in a Two layer Reinforced Soil System", *Computers and Geomechanics*, Vol.7, pp.19-36.
- BOUSSINESQ, J. (1885) : *Application des Potentiels a l'etude de l'equilibre et du Movement des Solids Elastiques*, Gauthier-Villars, Paris (in French).
- CHANDRA, S., MADHAV, M.R. and IYENGER, N.G.R. (1983) : "A New Model for Non-linear Subgrades", *4th Int. Conf. on Mathematical Modelling*, Zurich.
- CHEN, W.F. and BALADI, G.Y. (1985) : *Soil Plasticity : Theory and Implementation*, Elsevier, Amsterdam, p.231.
- DE COCK, F. and D'HOORE, S. (1994) : "Deep Soil Improvement by Rammed Stone Columns - Two Case Histories for large Diameter Storage Tanks", *Proc. 5th Int. Conf. on Piling and Deep Foundations*, Brugges, 5.21.1-5.21.9.
- EL-FADEL, M., FINDIKAKIS, A.N. and LECKIE, J.O. (1996) : "Biochemical and Physical Processes in Landfills", *Int. Jour. of Solid Waste Tech. and Management*, Vol.23, No.3, pp.131-143.
- FILONENKO-BORODICH, M.M. (1940) : "Some Approximate Theories of Elastic Foundations", *Uch. Zap. Mosk. Gos. Univ. Mekh.*, Vol.46, pp.3-18.
- GHOSH, C. (1991) : "Modelling and Analysis of Reinforced Foundation Beds", *Thesis* submitted in partial fulfillment for the degree of Ph.D., IIT. Kanpur.
- GHOSH, C. and MADHAV, M.R. (1994a) : "Reinforced Granular Fill - Soft Soil System : Membrane Effect", *Geotextiles and Geomembranes*, Vol.13, pp.743-759.
- GHOSH, C. and MADHAV, M.R. (1994b) : "Reinforced Granular Fill - Soft Soil System : Confinement Effect", *Geotextiles and Geomembranes*, Vol.13, pp.727-741.

- GHOSH, C. and MADHAV, M.R. (1994c) : "Settlement Response of a Reinforced Shallow Earth bed", *Geotextiles and Geomembranes*, Vol.13, pp.643-656.
- GIBSON, R.E. and LO, K.Y. (1961) : "A Theory of Consolidation of Soils Exhibiting Secondary Compression", *Norwegian Geotech. Inst. Publication No.41*, p.16.
- GIROUD, J.P. and NOIRAY, L. (1981) : "Geotextile Reinforced Unpaved Road Design", *J. Geotech. Engrg.*, ASCE, Vol.107, No.GT9, pp.1233-54.
- HARDIN, B.O. and DRNVICH, V.P. (1972) : "Shear Modulus and Damping in Soils : Measurement and Parameter Effects", *J. Soil Mech. & Found. Div.*, ASCE, Vol.98, No.SM6, pp.603-624.
- HETENYI, M. (1946) : *Beams on Elastic Foundations*, Univ. of Michigan Press, Ann Arbor.
- HOULSBY, G.T., MILLIGAN, G.V.E., JEWELL, R.A. and BURD, H.J. (1989) : "A New Approach to the Design of Unpaved Roads - Part I", *Ground Engineering*, Vol.23(3), pp.25-29.
- KAMESWARA RAO, N.S.V., DAS, Y.C. and ANADAKRISHNAN, M. (1971) : "Variational Approach to Beams on Elastic foundations", *Proc. ASCE*, Vol.97, No.EM2, pp.271-294.
- KERISEL, J. (1972) : "The Language of Models in Soil Mechanics", *Proc. 5th EC SMFE*, Madrid, Vol.II, pp.1-49.
- KERR, A.D. (1964) : "Elastic and Visco-elastic Foundation Models", *Jour. of Applied Mechanics*, Vol.31, No.3, pp.491-498.
- KERR, A.D. (1965) : "A Study of a New Foundation Model", *Acta Mechanica*, Vol.1, No.2, pp.134-147.
- LADE, P.V. (1977) : "Elasto-plastic Stress-Strain Theory for Cohesionless Soils with Curved Yield Surfaces", *Int. Jour. Solids and Structures*, Vol.13, No.4, pp.1325-1337.
- LADE, P.V. and DUNCAN, J.M. (1975) : "Elasto-plastic Stress-Strain Theory for Cohesionless Soils", *Jour. Geotech. Engrg.*, ASCE, Vol.101, No.GT10, pp.1037-1053.
- MADHAV, M.R. and DATYE, K.R. (1993) : "Bearing Capacity of Footings with Surcharge of Finite Extent", *Ind. Geotech. Jour.*, Vol.23, No.2, pp.277-284.
- MADHAV, M.R. and KAMESWARA RAO, N.S.V. and MADHAVAN, K. (1971) : "Laterally Loaded Pile in Elasto-Plastic Soil", *Soils and Foundations*, Vol.11, No.2, pp.1-15.
- MADHAV, M.R. and NAGPURE, D.D. (1995) : "Granular Piles -A Low Cost Alternative to RCC Piles", *National Workshop on Ground Improvement Techniques*, Indore, pp.17-30.
- MADHAV, M.R. and PITCHUMANI, N.K. (1992) : "Settlement Reduction due to Extensibic Reinforcement Strips", *Int. Symp. on Earth Reinf.*, IS Kyushu, Fukuoka, pp.631-636.
- MADHAV, M.R. and PITCHUMANI, N.K. (1994) : "Soil - Reinforcement Strip Interaction Analysis", *Computer Methods and Advances in Geomechanics*, edited by Siriwardane and Zaman, Vol.3, pp.1403-1408.

- MADHAV, M.R. and PITCHUMANI, N.K. (1996) : "Numerical Modelling and Analysis of Reinforced Strip - Soil Interaction", *11nd Int. Conf. in Civil Engrg. on Computer Applications - Research and Practice*, Bahrain, pp.579-588.
- MADHAV, M.R. and POOROOSHASB, H.B. (1987) : "Pasternak Concept for Modelling Soft Soil Overlain by Stiff Crust", *Proc. Ind. Geotech. Conf.*, Bangalore, Vol.1, pp.107-110.
- MADHAV, M.R. and POOROOSHASB, H.B. (1988) : "A New Model for Geosynthetic Reinforcement Soil", *Computers and Geotechnics*, Vol.6, pp.277-290.
- MADHAV, M.R. and POOROOSHASB, H.B. (1989) : "Modified Pasternak Model for Reinforced Soil", *Int. Jour. Mathematical Modelling*, Vol.12, No.12, pp.1505-1509.
- MADHAV, M.R. and SHARMA, J.S.N. (1991) : "Bearing Capacity of a Clay Overlain by a Stiff Soil", *Jour. Geotech. Engrg.*, ASCE, Vol.117, No.GT12, pp.1941-1948.
- MEYERHOF, G.G. (1974) : "Ultimate Bearing Capacity of Foundations on Sand Overlying Clay", *Canadian Geotech. Jour.*, Vol.11(2), pp.224-229.
- MILLIGAN, G.W.E., JEWELL, R.A., HOULSBY, G.T. and BURD, H.J. (1989) : "A New Approach to the Design of Unpaved Roads - Part I", *Ground Engineering*, Vol.22(8), pp.37-42.
- MIAO, T.D. and AI, N.S. (1988) : "Landslide Analysis and Prediction by Catastrophe Theory", *Int. Symp. on Landslides*, Lausanne, Vol.2, pp.731-733.
- MIURA, N. and MADHAV, M.R. (1994) : "Engineering of Ground in Lowlands", *Proc. Int. Symp. on Developments in Geotechnical Engineering from Harvard to New Delhi*, Bangkok.
- PASTERNAK, P.L. (1954) : "On a New Method of Analysis of an Elastic Foundation by Means of Two Foundation Constants", *Gos. Izd. Lit. po Stroit i Arkh.*, Moscow (in Russian).
- PITCHUMANI, N.K. (1992) : "Reinforced Foundation Beds : Soil - Reinforcement Interaction analysis", *Thesis* submitted in partial fulfillment for the degree of Ph.D., IIT, Kanpur.
- POOROOSHASB, H.B., PIETRUSZCZAK, S. and ASHTAKALA, B. (1985) : "An Extension of the Pasternak Foundation Concept". *Soil and Foundations*, Vol.25, No.3, pp.31-40.
- POULOS, H.G. and DAVIS, E.H. (1975) : *Elastic Solutions for Soil and Rock Mechanics*, John, Wiley & Sons, New York, p.411.
- POULOS, H.G. and DAVIS, E.H. (1980) : *Pile Foundation Analysis and Design*, John, Wiley & Sons, New York, p.411.
- RANDOLPH, M.F. and WROTH, C.P. (1978) : "Analysis of Deformation of Vertically Loaded Piles", *Jour. Geotech. Engrg.*, ASCE, Vol.104, pp.1465-1488.
- REISSNER, E. (1958) : "Deflection of Plates on Visco-elastic Foundations", *Jour. Applied Mech. Trans.*, ASME, Vol.80, No.3, p.144.
- RHINES, W.J. (1969) : "Elastic-plastic Foundation Model for Punch-Shear Failure", *Jour. of Soil Mech. and Found. Engrg. Div.*, ASCE, Vol.95, No.SM3, pp.819-828.

- SAITO, M. (1965) : "Predicting the Time of Occurrence of a Slope Failure", *Proc. 6th Int. Conf. SMFE*, Montreal, Vol.2, pp.537-541.
- SAXENA, S.K. and REDDY, K.R. (1989) : "Dynamic Moduli and Damping Ratios for Monterey Sand No. 0 Sand by Resonant Column Tests", *Soil and Foundations*, Vol.29, No.2, pp.37-51.
- SCHIFFMAN, R.L., LADD, C.C. and CHEN, A.T.F. (1964) : "The Secondary Consolidation of Clay", *Symp. on Rheology and Soil Mechanics*, p.126.
- SCOTT, R.F. (1981) : *Foundation Analysis*, Prentice-Hall Inc., Englewood, Cliffs., NJ, p.545.
- SHIVASHANKAR, R., MADHAV, M.R. and MIURA, N. (1993) : "Reinforced Granular Beds Overlying Soft Clay", *Proc. 11th SEAGC*, Singapore, pp.409-414.
- SHUKLA, S.K. and CHANDRA, S. (1994) : "A Study of Settlement Response of Geosynthetic Reinforced Compressible Granular Fill - Soft Soil System", *Geotextiles and Geomembranes*, Vol.13, No.9, pp.627-639.
- SHUKLA, S.K. and CHANDRA, S. (1995) : "Modelling of Geosynthetic Reinforced Engineered Granular Fill on Soft Soil", *Geosynthetic International*, Vol. 2, No.3, pp.603-617.
- TCHENG, Y. (1949) : *Poussée et Butée en Vraie Grandeur*, C.E.R.E.B.T.P., Paris.
- VLASOV, V.Z. (1949) : *Structural Mechanics of Thin Walled Three Dimensional System*, Gosstroizdat, Moscow (in Russian).
- VLASOV, V.Z. and LEONTEV, N.N. (1966) : *Beams, Plates and Shells on Elastic Foundations*, Translated from Russian by Israel Program of Scientific Translations, NTIS No. N67-14238.
- WINKLER, E. (1867) : *Die Lehre von der Elastizität und Festigkeit*, H. Dominicus, Prague (in German).
- YIN, J.H. (1997) : "Modelling Geosynthetic Reinforcement of Soft Soil under Pressure Loading", To appear in *Geosynthetics International*.